Statistical mechanics of nonuniform magnetization reversal

Hans-Benjamin Braun
Department of Physics, University of California San Diego, La Jolla, California 92093-0319
*and Department of Physics, Simon Fraser University, Burnaby, British Columbia, Canada V5A 1S6**
(Received 9 May 1994)

Thermally activated magnetization reversal in elongated particles is studied within a model that allows for spatially nonuniform magnetization configurations along the particle. An external field antiparallel to the existing magnetization is shown to give rise to an energy barrier which represents a spatially localized deviation from the initial uniform magnetization configuration. For sufficiently elongated particles, thermal fluctuations thus substantially lower the coercivity compared to the previous theories by Néel and Brown which assume a spatially uniform magnetization. The magnetization reversal rate is calculated using a functional Fokker-Planck description of the stochastic magnetization dynamics. Analytical results are obtained in the limits of small fields and fields close to the anisotropy field. In the former case the hard-axis anisotropy becomes effectively strong and the magnetization reversal rate is shown to reduce to the nucleation rate of kink-antikink pairs in the overdamped sine-Gordon model. The present theory therefore includes the nucleation theory of the double sine-Gordon chain as a special case.

I. INTRODUCTION

The magnetization in a uniformly magnetized sample is usually stabilized by an easy-axis anisotropy of crystalline or demagnetizing origin. To reach a state of zero net magnetization one has to apply an external field in the reversed direction, the so-called coercive field. In macroscopic samples of high purity such as yttrium iron garnet (YIG),[1] this field can be less than 10^{-2} Oe. This low coercivity is commonly attributed to the existence of residual domains of reverse magnetization in the original uniformly magnetized state. The measured coercivity is then associated with the depinning and motion of the corresponding domain walls.

This situation is strikingly different for microscopic single-domain particles where no such residual domains exist. The coercivity can reach values of more than 1000 Oe since the state of reversed magnetization has first to be nucleated. Consequently such particles exhibit an extremely high long-term stability of the magnetization. This fact renders them suitable for information storage in recording media and as constituents of rocks they preserve the value of the local magnetic field as the temperature has dropped below the blocking temperature of the particle. With decreasing sample size, however, the effect of thermal fluctuations becomes increasingly important. For particle sizes of a few nanometers and at room temperature the magnetization fluctuates randomly over the anisotropy barrier and a superparamagnetic state results with vanishing average magnetic moment.

This paper concentrates on particles whose size is above the superparamagnetic limit but which are still small enough that the coercivity is affected by thermal fluctuations. The only *ab initio* theory has been developed by Néel[2] and Brown[3] and it is based on the assumption that the magnetization distribution is uniform throughout the sample. Consequently the energy barrier is proportional to the volume and the Arrhenius factor leads to an exponential suppression of thermal effects with the particle volume. This picture is indeed adequate for small particles of approximately spherical shape. However, for sufficiently elongated particles a magnetization reversal via a rigid rotation of the magnetization becomes energetically unfavorable. It will be more advantageous to form a spatially localized excursion from the metastable state since the additional cost of exchange energy due to the spatial nonuniformity is by far outweighed by the gain of anisotropy energy by keeping the deviation localized.

It is the purpose of this paper to formulate an *ab initio* theory of this effect and to show that for sufficiently elongated particles a spatially nonuniform barrier yields a much lower coercivity than previous theories. A short account of the results of the present paper has already been given elsewhere.[4] We shall start from a classical one-dimensional (1D) model energy density which takes into account the exchange interaction between the magnetic moments along the particle. In addition, the energy density contains hard- and easy-axis anisotropies as well as the coupling to an external field. The anisotropies may contain contributions of both shape and crystalline anisotropies. The barrier energy is then shown to be independent of the hard-axis anisotropy, and it is proportional to the domain-wall energy and the sample cross sectional area. Consequently, the barrier energy is independent of the particle length for sufficiently elongated particles.

In order to induce magnetization reversal, thermal fluctuations have to form a "nucleus" of critical size with the property that smaller deformations fall back to the metastable state whereas larger deformations grow with energy gain until the magnetization is reversed. There-

fore the nucleus represents an unstable structure with exactly one unstable mode. An analytical expression for this structure has been obtained[4,5] and the spin-wave excitations of the nucleus have been investigated in a previous paper[6] (henceforth referred to as I). For external fields close to the anisotropy field which renders an individual magnetic moment unstable, the nucleus represents only a small deviation from the metastable state. For small fields, the nucleus consists of two well-separated domain walls enclosing an already reversed domain.

The present approach relies on methods that have been used in the description[7] of the dynamics of first-order phase transitions. This method has been applied for the description of the decay of a supercurrent[8] in a thin wire or the propagation[9,10] of dislocations. In contrast to these applications we consider here the regime of moderate damping since damping in magnetic systems is very small. The rate is shown to be the product of a prefactor depending on the external field and temperature T, and the Arrhenius factor $\exp\{-\mathcal{A}\mathcal{E}_s/k_BT\}$ which involves the barrier energy $\mathcal{A}\mathcal{E}_s$ with $\mathcal{A}$ the sample cross sectional area (k_B is the Boltzmann constant).

For the evaluation of the prefactor we shall employ two different approaches. One is the Jacobi method which relies on the explicit knowledge of a zero energy (Goldstone) mode. Therefore it can only be applied for easy-plane fluctuations but it cannot be used for out of easy-plane excitations due to the existence of a mass gap. The second method makes use of the scattering phase shifts of spin waves around the nucleus. This latter approach reveals some considerable subtleties which do not seem to have been noted previously. First, for even-parity wave functions the 1D version[11,12] of Levinson's theorem alters the usual expression for the density of states. Second, the number of bound states of the fluctuation operators is not conserved under small and large nucleus approximations. This fact raises doubts about the commonly employed approach of performing functional integrals of the free energy after already having performed the limits of small or large nuclei. By a careful investigation it is shown that these two subtleties conspire in such a way that this interchange of limits is indeed legitimate.

There are only sparse treatments of magnetization reversal in the literature. However, this field is closely related to macroscopic quantum tunneling of the (sublattice) magnetization in small (anti)ferromagnetic grains, a subject that has attracted much interest recently. It thus appears to be useful to relate some important papers that contributed to the development of these fields.

Early work on nucleation theory culminated in the celebrated paper[13] by Kramers who calculated the escape rate due to thermal activation out of a metastable state in the limits of low as well as moderate to large friction. He showed that the rate is given by a prefactor times the Arrhenius term. Despite the fact that his work was restricted to systems with one degree of freedom, his method of the evaluation of the prefactor turned out to be so powerful that its spirit still underlies much more complex applications. An extension to an arbitrary number of degrees of freedoms in the large friction limit was due to Brinkman,[14] and Landauer-Swanson and Langer.[14] The case of moderate friction has been considered by Langer[7] who also pointed out that the nucleation rate may be interpreted as the analytic continuation of the partition function. This idea is closely related to the subsequently developed instanton concept[15] in Euclidean quantum field theories. Kramers's theory and its extensions have recently been reviewed by Hänggi, Talkner, and Borkovec.[16]

The first application of Kramers' theory to magnetic systems has been made by Brown[3] who investigated thermally activated uniform magnetization reversal in small ferromagnetic particles to explain superparamagnetism. He set up the Fokker-Planck equation for the stochastic dynamics of the magnetization and thus related Néel's earlier considerations[2] on reversal rates with the general framework of statistical mechanics. For axial symmetry of the anisotropy he obtained nucleation rates from the lowest nonzero eigenvalue of the Fokker-Planck equation in the limit of low barriers. For a high barrier he used Kramers' procedure to evaluate the rate constant. Later the lowest positive eigenvalue was investigated numerically for all intermediate values between low and large barriers by Aharoni.[17] Eisenstein and Aharoni[18] investigated the competition of the uniform mode and the nonuniform curling mode as possible candidates of critical nuclei for different particle radii. However, the nucleation rates via the nonuniform mode were calculated using Brown's theory[3] for spatially uniform nucleation.

Subsequently the issue of magnetization reversal rates was not addressed for many years. A renewal of interest then arose from a quantum mechanical point of view. Based on path integral[19] and WKB (Ref. 20) techniques, first investigations showed that a single spin in an anisotropic field behaves similar to a particle with inertia and tunnels between different anisotropy minima. It has then been suggested[21] that in small ferromagnetic particles macroscopic quantum tunneling might occur. The effect of dissipation due to magnetoelastic coupling has been discussed by Garg and Kim.[22] In the context of recent experiments[23] these approaches have been reexamined and it has been predicted[24] that quantum tunneling is suppressed for half-integer spins as a consequence of a previously neglected Wess-Zumino term in the quantum spin action and the destructive interference of instanton and anti-instanton paths.

While all these approaches dealt with tunneling via spatially uniform structures, tunneling via spatially nonuniform (bubble) structures in two dimensions was investigated in the limit of external magnetic fields close to the anisotropy field[25] and for very small fields in the thin wall approximation.[26] In the latter case the nucleating structure is a large cylindrical domain of reversed magnetization delimited by a Bloch wall. Various aspects of quantum tunneling with emphasis on tunneling of Bloch walls have recently been reviewed by Stamp, Chudnovsky, and Barbara.[27]

Surprisingly, the conceptually much simpler classical problem of thermal nucleation remained untouched until recently. Klik and Gunther[28] calculated the nucleation rate for nucleation via uniform structures for cubic symmetry. In contrast to earlier investigations they also

calculated nucleation rates for a weakly damped system. Nuclei of curling symmetry[29] in an infinite cylinder[30] and a nucleation center of spherical symmetry[31] have been investigated recently.

From this review, there emerges clearly the need of an *ab initio* theory for magnetization reversal rates via spatially nonuniform structures. The present work is organized as follows.

In Sec. II some results of paper I are reviewed which are relevant to the present work. In Sec. III a functional Fokker-Planck equation is constructed which describes the stochastic magnetization dynamics near the nucleus and the corresponding nucleation rate is derived. It is shown that the result has the same general structure as that of Ref. 7(b). The prefactor separates into a term describing the dynamical decay of the nucleus and in a term arising from the Gaussian fluctuations around the nucleus. The unstable mode enters in such a way as if it represented a stable mode. The details of the calculations are presented in the Appendix. The explicit evaluation of the prefactors in various limits is then the subject of the remaining sections. In Sec. IV we evaluate the statistical part of the prefactor analytically in the limit of small and large nuclei as well as for large and small values of the hard-axis anisotropy. For small nuclei and if the hard-axis anisotropy is much larger than the easy-axis anisotropy, the out-of-easy-plane fluctuations do not contribute at all. In Sec. V the nucleation rate is evaluated in the overdamped limit. The rate in the moderately damped regime and the decay frequency of the nucleus are investigated in Sec. VI. In Sec. VII the results of the previous sections are used to calculate the creation rate of kink-antikink pairs in the double sine-Gordon system. It is shown that this rate reproduces the magnetization reversal rate in the limit of large hard-axis anisotropy or external fields close to the (easy-axis) anisotropy field. In Sec. VIII experimental implications are discussed. For a particle of 100 Å diameter and an aspect ratio 15 : 1, the present theory is shown to yield a coercivity reduction from the anisotropy field that is twice as large as that of the Néel-Brown theory. Finally the applicability range of the present theory is discussed since it is known that in the underdamped limit the rate is governed by a diffusion in energy rather than in configuration space.

II. MODEL, NUCLEUS, AND FLUCTUATIONS

In this section we present the model and review some important results of paper I. The ferromagnet is described within a classical continuum model, the magnetization being represented by a vector $\mathbf{M}$ of constant magnitude M_0. We focus on an effectively one-dimensional situation where the magnetization only depends on one coordinate, i.e., $\mathbf{M} = \mathbf{M}(x,t)$. The energy per unit area is given by

$$\mathcal{E} = \int_{-L/2}^{L/2} dx \left\{ \frac{A}{M_0^2} \left[(\partial_x M_x)^2 + (\partial_x M_y)^2 + (\partial_x M_z)^2 \right] - \frac{K_e}{M_0^2} M_x^2 + \frac{K_h}{M_0^2} M_z^2 - H_{\rm ext} M_x \right\}, \tag{2.1}$$

where $\partial_x \equiv \partial/\partial x$ and L is the finite sample length in the x direction. Ultimately, we shall be interested in the limit $L \to \infty$. The first term in (2.1) is the classical counterpart of the exchange energy and A is an exchange constant. The second term defines an easy axis along the x direction. The third term is a hard-axis anisotropy which favors the magnetization to lie in the xy plane. $K_e > 0$ and $K_h > 0$ are easy- and hard-axis anisotropy constants, respectively. The degeneracy between the two anisotropy minima along the x axis is lifted by an external magnetic field $H_{\rm ext}$ along the positive x axis. The energy (2.1) describes magnetization configurations in an elongated particle of diameter smaller[32] or comparable to the minimal length scale in the system $\sqrt{A/K_{\rm max}}$, where $K_{\rm max}$ is the larger of the anisotropy constants K_e, K_h.

Note that the energy (2.1) can be used to describe three distinct anisotropy configurations in elongated particles. The first, most common case is an easy axis along the particle axis which may be caused by both demagnetizing (shape) and crystalline anisotropy [cf. Fig. 1(a)]. E.g., for an infinite cylinder with an easy axis along the sample one has $K_e = \pi M_0^2 + K_{e,\rm cryst}$ where the first term is due to the shape anisotropy and the second term due to crystalline anisotropy. The hard-axis anisotropy may arise either from an additional crystalline easy axis that is misaligned with the particle axis or from an elliptic sample cross section. The second case is an elongated particle of a material of high crystalline anisotropy ($K_{e,\rm cryst} > 2\pi M_0^2$) with both easy and hard axes perpendicular to the long axis of the sample [cf. Fig. 1(b)]. The third case refers to a thin slab with an easy-axis anisotropy in the film plane [cf. Fig. 1(c)].

In the following we focus on a situation as in Fig. 1(a). The results for configurations shown in Figs. 1(b) and 1(c) are simply obtained by substituting y and z for the x dependence of the magnetization. The components in internal (spin) space remain unchanged and the spherical coordinates are always defined in the same way with

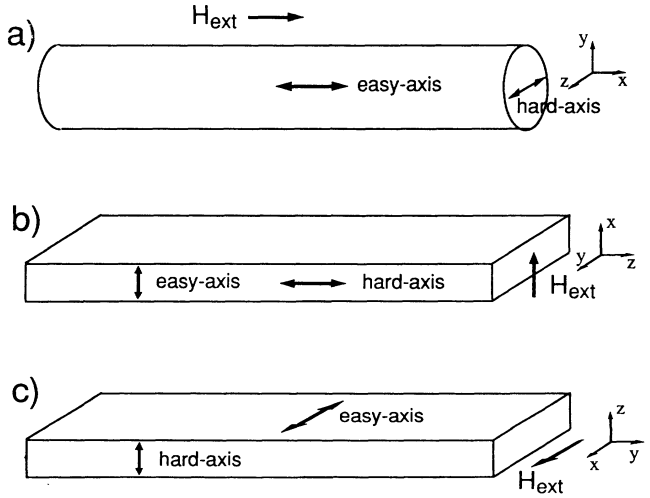

FIG. 1. Various anisotropy configurations axes that can be described by the energy density (2.5). The sample cross sectional areas are assumed to be sufficiently small such that transversal variations in the magnetization are suppressed.

respect to the coordinate axes.

The dissipative dynamics of the magnetization is assumed to obey the Landau-Lifshitz-Gilbert equations (see, e.g., Ref. 33):

$$\partial_t \mathbf{M} = -\gamma \mathbf{M} \times \mathbf{H}_{\text{eff}} + \frac{\alpha}{M_0} \mathbf{M} \times \partial_t \mathbf{M}, \tag{2.2}$$

where $\gamma > 0$ denotes the gyromagnetic ratio, $\alpha > 0$ is the dimensionless damping constant, and $\partial_t = \partial/\partial t$. The first term on the (right-hand side) of (2.2) describes the precession of the magnetization in the effective magnetic field $\mathbf{H}_{\text{eff}} = -\delta\mathcal{E}/\delta\mathbf{M}$ ($\delta/\delta\mathbf{M}$ denotes a functional derivative). The second term in (2.2) is a viscous damping term and accounts for the relaxation of the magnetization into the direction of the effective magnetic field. This term is phenomenological in nature. It describes damping processes which conserve the magnitude of the magnetization at every space point. It is convenient to rewrite (2.2) as follows:

$$(1+\alpha^2)\partial_t \mathbf{M} = -\gamma \mathbf{M} \times \mathbf{H}_{\text{eff}} - \frac{\alpha\gamma}{M_0} \mathbf{M} \times [\mathbf{M} \times \mathbf{H}_{\text{eff}}]. \tag{2.3}$$

This equation is obtained by evaluating the cross product of $\mathbf{M}$ with (2.2). Equation (2.3) is similar to the damping term originally proposed by Landau and Lifshitz. However, Eq. (2.3) contains the damping parameter α such that the motion is slowed down for large α while the original equation of Landau-Lifshitz exhibits an unphysical acceleration of the motion for large damping parameters.

Since (2.3) conserves the magnitude of the magnetization, it is appropriate to introduce spherical coordinates according to $\mathbf{M}/M_0 = (\sin\theta\cos\phi, \sin\theta\sin\phi, \cos\theta)$. We use dimensionless units defined by

$$\begin{aligned} [x] &= [y] = [z] = \sqrt{\frac{A}{K_e}}, \\ [t] &= (1+\alpha^2)\frac{M_0}{2\gamma K_e}, \\ [\mathcal{E}] &= 2\sqrt{AK_e}. \end{aligned} \tag{2.4}$$

$\sqrt{A/K_e}$ is the Bloch-wall width, $2\gamma K_e/M_0$ is the precession frequency in the anisotropy field. To simplify notation, an additional factor $1+\alpha^2$ has been absorbed in the time scale. $2\sqrt{AK_e}$ is half the energy of a static π-Bloch wall. In dimensionless units and spherical coordinates the energy per area (2.1) takes the form

$$\begin{aligned} \mathcal{E} = \int_{-L/2}^{L/2} dx \Big\{ & \frac{1}{2}\left[(\partial_x\theta)^2 + \sin^2\theta(\partial_x\phi)^2\right] \\ & -\frac{1}{2}[\sin^2\theta\cos^2\phi - 1] + \frac{Q^{-1}}{2}\cos^2\theta \\ & -h[\sin\theta\cos\phi + 1]\Big\}. \end{aligned} \tag{2.5}$$

In (2.5), the dimensionless anisotropy ratio

$$Q = \frac{K_e}{K_h} \tag{2.6}$$

and the reduced external field

$$h = \frac{H_{\text{ext}} M_0}{2K_e} \tag{2.7}$$

have been introduced. Using (2.4) and spherical coordinates, the equations of motion (2.3) take the form (see also the Appendix of Ref. 33)

$$\begin{aligned} \sin\theta\,\partial_t\phi &= \frac{\delta\mathcal{E}}{\delta\theta} - \alpha\frac{1}{\sin\theta}\frac{\delta\mathcal{E}}{\delta\phi}, \\ \partial_t\theta &= -\frac{1}{\sin\theta}\frac{\delta\mathcal{E}}{\delta\phi} - \alpha\frac{\delta\mathcal{E}}{\delta\theta}. \end{aligned} \tag{2.8}$$

The first terms on the rhs describe the precession in the effective magnetic field, whereas the terms proportional to α are damping terms.

Spatially uniform static solutions of (2.3) lie in the easy plane and are given by $(\phi_0, \theta_0) = (0, \pi/2)$ and $(\phi_m, \theta_m) = (\pi, \pi/2)$, the latter being stable only for $h < 1$. The state (ϕ_0, θ_0) is completely aligned with the external field and thus represents the state of lowest energy. The configuration (θ_m, ϕ_m) is oriented antiparallel to the external field and its energy per volume exceeds that of the ground state (ϕ_0, θ_0) by $2h$. Therefore (θ_m, ϕ_m) is a metastable state for $h < 1$.

At finite temperatures, the magnetization exhibits fluctuations around the metastable state until it eventually overcomes a barrier for magnetization reversal. For large sample lengths L, a magnetization reversal via a uniform rotation of the magnetization is highly unlikely since it would require an energy proportional to L. Instead, the system will establish magnetization reversal by forming a spatially localized deviation from the metastable state. There is a well-defined "nucleus" of critical size with the property that deformations of smaller size fall back to the metastable state, whereas larger deformations grow with energy gain until the whole system is in the ground state parallel to the external field. In paper I it has been shown that the magnetization configuration [cf. (3.9 of I)] defined by

$$\tan\frac{\phi_s^{\pm}}{2} = \pm\frac{\cosh\frac{x-x_0}{\delta}}{\sinh R}, \qquad \theta_s = \pi/2, \tag{2.9}$$

with

$$\operatorname{sech}^2 R = h, \qquad \delta = \coth R, \tag{2.10}$$

exhibits exactly one unstable mode and thus represents such a nucleus of critical size. Equation (2.9) is in principle only valid for a sample of infinite length L but it is an excellent approximation for a sample of finite length if $L > 2\pi\sqrt{A/K_e}$. For simplicity the subscript s of δ and R has been dropped in contrast to paper I. x_0 denotes the arbitrary position of the nucleus along the particle. This degeneracy with respect to translations gives rise to a zero energy (Goldstone) mode. In the following we shall put $x_0 = 0$. The structure (2.9) can also be viewed as a superposition of two π-Bloch walls centered at $x = \pm R/\delta + x_0$ with opposite relative sense of twist. For R small, (2.9) represents only a small deviation from the metastable state, whereas for large R it represents a

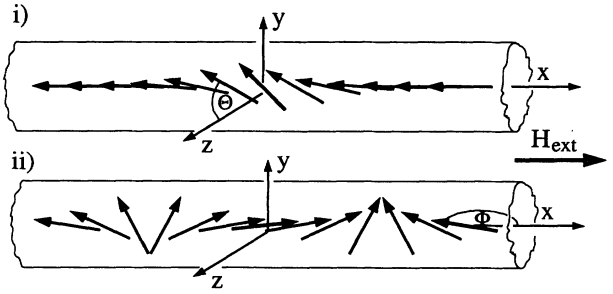

FIG. 2. The spatial variation of the nucleus is shown for (i) fields close to the anisotropy field and (ii) small fields. In these pictures, the magnetic chain is taken along the easy axis. However, the model (2.5) equivalently applies to all situations shown in Fig. 1.

large domain of size $2R\delta$ delimited by an untwisted pair of domain walls (cf. Fig. 2). In the following we shall restrict ourselves to ϕ_s^+ only and we shall drop the superscript. The existence of two equivalent saddle points will result in a factor of 2 in the final expression of the nucleation rate.

Out-of-easy-plane fluctuations p and azimuthal fluctuations φ around ϕ_s are introduced as follows:

$$\begin{aligned}\phi(x,t) &= \phi_s(x) + \varphi(x,t),\\ \theta(x,t) &= \pi/2 - p(x,t).\end{aligned} \tag{2.11}$$

Inserting (2.11) into the energy (2.5) we obtain up to second order in φ and p

$$\mathcal{E}_s^{(2)} = \mathcal{E}_s + \frac{1}{2}\int_{-L/2}^{L/2} dx\, \varphi\, \mathcal{H}^{s\varphi}\, \varphi + \frac{1}{2}\int_{-L/2}^{L/2} dx\, p\, \mathcal{H}^{sp}\, p, \tag{2.12}$$

where

$$\mathcal{H}^{s\varphi} = -\frac{d^2}{dx^2} + \delta^{-2} V_-\left(\frac{x}{\delta}, R\right), \tag{2.13}$$

$$\mathcal{H}^{sp} = -\frac{d^2}{dx^2} + \delta^{-2} V_+\left(\frac{x}{\delta}, R\right) + Q^{-1}. \tag{2.14}$$

The energy per unit area of the nucleus (2.9) is given by

$$\mathcal{E}_s = 4\tanh R - 4R\,\mathrm{sech}^2 R. \tag{2.15}$$

The characteristic width δ is given by (2.10), and the potentials $V_\pm$ can be inferred from (4.13) of paper I:

$$\begin{aligned}V_\pm(\xi, R) = 1 &- 2\,\mathrm{sech}^2(\xi + R) - 2\,\mathrm{sech}^2(\xi - R)\\ &\pm 2\,\mathrm{sech}(\xi + R)\,\mathrm{sech}(\xi - R).\end{aligned} \tag{2.16}$$

The eigenvalue problems of (2.13) and (2.14) are written as follows:

$$\mathcal{H}^{s\varphi}\chi_\nu^{s\varphi}(x,R) = E_\nu^{s\varphi}(R)\chi_\nu^{s\varphi}(x,R), \tag{2.17}$$

$$\mathcal{H}^{sp}\chi_\nu^{sp}(x,R) = E_\nu^{sp}(R)\chi_\nu^{sp}(x,R), \tag{2.18}$$

where ν denotes both bound states and scattering states. From I, two solutions of the eigenvalue problems (2.17) are known: the ground state of $\mathcal{H}^{sp}$,

$$\chi_0^{sp} \propto \delta^{-1}\left\{\mathrm{sech}\left(\frac{x}{\delta} + R\right) + \mathrm{sech}\left(\frac{x}{\delta} - R\right)\right\}, \tag{2.19}$$

$$E_0^{sp} = Q^{-1},$$

and the first excited state of $\mathcal{H}^{s\varphi}$,

$$\chi_1^{s\varphi} \propto \delta^{-1}\left\{\mathrm{sech}\left(\frac{x}{\delta} + R\right) - \mathrm{sech}\left(\frac{x}{\delta} - R\right)\right\}, \quad E_1^{s\varphi} = 0. \tag{2.20}$$

Since $\chi_1^{s\varphi}$ is antisymmetric, there is exactly one unstable mode of negative energy in φ while all fluctuations in the p-direction have positive energy since $Q^{-1} > 0$. Therefore the untwisted domain-wall pair represents a saddle point of the energy with exactly one unstable direction.

The operators characterizing the modes around the metastable state (ϕ_m, θ_m) are obtained in an analogous way. Inserting

$$\begin{aligned}\phi(x,t) &= \pi + \varphi(x,t),\\ \theta(x,t) &= \pi/2 - p(x,t),\end{aligned} \tag{2.21}$$

into (2.5) we have

$$\mathcal{E}_m^{(2)} = \frac{1}{2}\int_{-L/2}^{L/2} dx\, \varphi\, \mathcal{H}^{m\varphi}\, \varphi + \frac{1}{2}\int_{-L/2}^{L/2} dx\, p\, \mathcal{H}^{mp}\, p, \tag{2.22}$$

where the operators

$$\begin{aligned}\mathcal{H}^{m\varphi} &= -\frac{d^2}{dx^2} + \delta^{-2},\\ \mathcal{H}^{mp} &= -\frac{d^2}{dx^2} + \delta^{-2} + Q^{-1}\end{aligned} \tag{2.23}$$

reflect the spatial uniformity of the metastable state. In order to calculate nucleation rates by thermal activation, we have to examine the stochastic dynamics around the nucleus.

III. STOCHASTIC MOTION AND NUCLEATION RATE

The dissipative dynamics of the magnetization is governed by the equations of motion (2.8). To investigate the dynamics near the nucleus, we insert (2.11) and (2.12) into (2.8) and obtain the linearized equations of motion

$$\begin{aligned}\partial_t\varphi &= -\mathcal{H}^{sp}p - \alpha\mathcal{H}^{s\varphi}\varphi,\\ \partial_t p &= \mathcal{H}^{s\varphi}\varphi - \alpha\mathcal{H}^{sp}p.\end{aligned} \tag{3.1}$$

Notice the unusual occurrence of damping terms proportional to α in the equations of motion for both φ and p. The reversible part of (3.1) is of Hamiltonian structure. This is due to the fact that the z component of the angular momentum $\cos\theta$ and the azimuthal angle ϕ are canonically conjugate variables. However, the signs

in Eq. (3.1) are reversed compared to a usual canonical theory since we are dealing with the magnetization rather than the angular momentum.

The statically unstable mode has a dynamical counterpart $(\varphi_+(x,t),p_+(x,t)) \propto e^{\lambda_+ t}(\varphi_+(x),p_+(x))$ with $\lambda_+ > 0$ which inserted into (3.1) obeys the coupled eigenvalue problem

$$\begin{aligned}\lambda_+\varphi_+ &= -\mathcal{H}^{sp}p_+ - \alpha\mathcal{H}^{s\varphi}\varphi_+,\\ \lambda_+p_+ &= \mathcal{H}^{s\varphi}\varphi_+ - \alpha\mathcal{H}^{sp}p_+,\end{aligned} \tag{3.2}$$

with the boundary conditions $\varphi_+(\pm\frac{L}{2}) = p_+(\pm\frac{L}{2}) = \varphi'_+(\pm\frac{L}{2}) = p'_+(\pm\frac{L}{2}) = 0$. The linearized equations of motion (3.1) can also be cast in a compact form

$$\partial_t\psi_i(x,t) = -\sum_j M_{ij}\mathcal{H}_j\psi_j(x,t). \tag{3.3}$$

In (3.3) we have introduced

$$\psi(x,t) \equiv (\varphi(x,t),p(x,t)) \tag{3.4}$$

and the dynamic matrix

$$M = \begin{pmatrix} \alpha & 1 \\ -1 & \alpha \end{pmatrix}, \tag{3.5}$$

which is the sum of a symplectic matrix describing the reversible part of the dynamics and a diagonal positive definite dissipative matrix. For the operators in (3.3) we have used the notation $(\mathcal{H}_1,\mathcal{H}_2) \equiv (\mathcal{H}^{s\varphi},\mathcal{H}^{sp})$.

Equation (3.3), and equivalently (3.1), describes the deterministic motion of the system in the vicinity of the saddle point. However, it is not consistent with the fluctuation dissipation theorem since it lacks the stochastic forces resulting from the coupling to the heat bath. Without these stochastic forces, the magnetization would never be driven away from the initial metastable state. Stochastic forces can be added to the rhs of (3.1) or (3.3) to yield the Langevin equation

$$\partial_t\psi_i(x,t) = -\sum_j M_{ij}\mathcal{H}_j\psi_j(x,t) + \zeta_i(x,t)\ , \tag{3.6}$$

where ζ_i is Gaussian white noise with $\langle\zeta_i\rangle = 0$ and

$$\langle\zeta_i(x,t)\zeta_j(x',t')\rangle = \frac{2\alpha}{\beta\mathcal{A}}\delta_{ij}\delta(x-x')\delta(t-t')\ , \tag{3.7}$$

where $\langle\cdots\rangle$ denotes the average with respect to the Gaussian noise distribution $\exp\{-\beta\mathcal{A}/(4\alpha)\int dt\,dx\sum_i\xi_i^2\}$ and $\beta = 1/k_BT$. The dynamics of the probability distribution functional $\varrho[\psi(x)] = \langle\prod_{i,x}\delta(\psi_i(x,t)-\psi_i(x))\rangle$ with $\psi_i(x,t)$ a solution of (3.6) is governed[38] by the Fokker-Planck equation

$$\partial_t\varrho[\psi(x)] = -\int dx\sum_i\frac{\delta J_i}{\delta\psi_i(x)}. \tag{3.8}$$

The probability current is given by

$$J_i = -\sum_j M_{ij}\left[\mathcal{H}_j\psi_j(x) + \frac{1}{\beta\mathcal{A}}\frac{\delta}{\delta\psi_j(x)}\right]\varrho[\psi(x)]. \tag{3.9}$$

In (3.9) we have exploited the antisymmetry of the off-diagonal part of M. Note that the current is only defined up to a divergenceless term. If we demand in addition that the equilibrium density have vanishing current, the representation (3.9) is unique. Equations (3.8) and (3.9) have the following properties:

(i) The equations of motion for the thermal expectation values $\langle\varphi\rangle$,$\langle p\rangle$ are identical to the expectation value of (3.3). (Expectation values are defined by $\langle\varphi\rangle = \int\mathcal{D}\varphi\mathcal{D}p\,\varphi\,\varrho$, where $\int\mathcal{D}\varphi$ denotes functional integration.)

(ii) The equilibrium density near the saddle point,

$$\varrho_{\rm eq} = Z^{-1}\exp\{-\beta\mathcal{A}\mathcal{E}_s^{(2)}\}, \tag{3.10}$$

with $\mathcal{E}_s^{(2)}$ as in (2.12), is a stationary solution of (3.8) with vanishing current. Z is a normalization constant arising from the condition that $\int\mathcal{D}\varphi\mathcal{D}p\,\varrho_{\rm eq} = 1$ in the vicinity of the metastable state. Since $\varrho_{\rm eq}$ is sharply peaked around the metastable state, a Gaussian approximation may be used for the evaluation of Z. Note that the properties (i), (ii) also allow for a direct construction of the Fokker-Planck equation without making use of the Langevin equation.

To calculate the nucleation rate, we have to construct a stationary nonequilibrium probability density. To maintain a constant probability flux over the saddle point we impose the boundary conditions $\varrho \simeq \varrho_{\rm eq}$ near the metastable state and $\varrho \simeq 0$ beyond the saddle point. Note that the realization of equilibrium at the metastable state requires a barrier energy which should be large compared to thermal energies. As a criterion we may use $\beta\mathcal{A}\mathcal{E}_s \gtrsim 5$. Since the prefactor is roughly of the order of the precession frequency $2\gamma K_e/M_0 \simeq 10^{10}\ {\rm s}^{-1}$, this inequality is satisfied even for very large switching rates and thus does not represent a restriction. The total rate is then obtained as the probability flux integrated across a surface transversal to the unstable mode. The derivation is similar to that of Langer[7] and is presented in detail in the Appendix. The switching probability per unit time of a particle with magnetization prepared in the metastable state into the stable state is then given by

$$\Gamma = \Omega e^{-\beta\mathcal{A}\mathcal{E}_s}, \tag{3.11}$$

where $\mathcal{A}$ is the cross sectional area of the sample and $\mathcal{E}_s$ is the energy (2.15) per area of the nucleus. The prefactor is given as follows:

$$\Omega = \lambda_+\mathcal{L}\sqrt{\frac{\beta\mathcal{A}}{2\pi^3}}\sqrt{\frac{\det\mathcal{H}^{m\varphi}}{\det'|\mathcal{H}^{s\varphi}|}}\sqrt{\frac{\det\mathcal{H}^{mp}}{\det\mathcal{H}^{sp}}}. \tag{3.12}$$

In (3.12) an explicit factor of 2 has been included, since the metastable state $\phi = \pi,\theta = \pi/2$ may decay via either one of the two equivalent saddle points $\phi_\pm$. The first factor on the rhs of (3.12) is the escape frequency of the unstable mode as defined by (3.2). This is the only term in (3.12) in which dynamical details of the system enter. The second factor arises from the integration over the zero frequency (Goldstone) mode and is defined by $\mathcal{L} = \sqrt{\mathcal{E}_s}L$, where L is the system length and $\mathcal{E}_s$ is the

energy per unit area (2.15). The third factor is also due to the Goldstone mode and determines the temperature dependence of the prefactor. The remaining factors basically arise from the functional integration of the partition function within Gaussian approximation (2.12) and (2.22). The determinants are defined as the products of eigenvalues,

$$\frac{\det \mathcal{H}^{m\varphi}}{\det' |\mathcal{H}^{s\varphi}|} = \frac{\prod_k E_k^{m\varphi}}{|E_0^{s\varphi}| E_2^{s\varphi} \prod_{k'} E_{k'}^{s\varphi}}, \tag{3.13}$$

where k denotes scattering states. The prime on det denotes omission of the zero energy $E_1^{s\varphi}$. However, note that the unstable mode $E_0^{s\varphi} < 0$ enters (3.13) as if it were a stable one. The determinant of out of easy-plane fluctuations is defined as

$$\frac{\det \mathcal{H}^{mp}}{\det \mathcal{H}^{sp}} = \frac{\prod_k E_k^{mp}}{E_0^{sp} E_1^{sp} \prod_{k'} E_{k'}^{sp}}. \tag{3.14}$$

The bound state energies $E_0^{s\varphi}$ and E_1^{sp} are given by (2.19) and (2.20). In paper I we obtained $E_2^{s\varphi} \simeq \delta^{-2}$ [(6.13) of paper I] and $E_0^{s\varphi}$ and E_1^{sp} have been evaluated numerically for arbitrary R.

Therefore we are left with the task of evaluating the products of the continuum eigenvalues. The continuum eigenvalues of $\mathcal{H}^{s\varphi}$ and $\mathcal{H}^{sp}$ coincide with those of $\mathcal{H}^{m\varphi}$ and $\mathcal{H}^{mp}$, respectively, and are given by

$$\begin{aligned} E_k^{m\varphi} &= E_k^{s\varphi} = \delta^{-2} + k^2, \\ E_k^{mp} &= E_k^{sp} = Q^{-1} + \delta^{-2} + k^2. \end{aligned} \tag{3.15}$$

Note that these equalities do not imply a cancellation of numerators and denominators in (3.13) and (3.14), since the allowed k values are different and fixed by the boundary conditions which we choose as periodic.

The next sections are devoted to the explicit evaluation of the infinite products (3.13), (3.14) and the calculation of the escape frequency λ_+.

IV. EVALUATION OF THE STATISTICAL PREFACTOR

In the following we describe two methods for the evaluation of the statistical prefactors (3.13), (3.14).

The first method (see, e.g., Ref. 35) is based on the knowledge of scattering phase shifts of the continuum eigenfunctions as well as the bound state energies of the operators $\mathcal{H}^{s\varphi}$, $\mathcal{H}^{sp}$. In strictly one-dimensional problems one has to distinguish between the scattering phase shifts of odd- and even-parity wave functions. This is in sharp contrast to the familiar situation of a 3D s-wave scattering problem where the scaled wave function indeed obeys a 1D Schrödinger equation but is required to vanish at the origin. Surprisingly, this issue has been ignored until recently,[11,12] possibly also due to the fact that the most widely used 1D potentials belong to the rather special class of reflectionless potentials for which scattering phase shifts of even and odd wave functions coincide.

So far, the present method for the evaluation of the prefactor has indeed been used only[35] in the case of reflectionless potentials where the scattering phase shifts of even and odd wave functions coincide. Here, however, the potentials in $\mathcal{H}^{s\varphi}$ and $\mathcal{H}^{sp}$ only become reflectionless in the limits $R \to 0$ and $R \to \infty$. For intermediate values of R, the corresponding potentials are not reflectionless and scattering phase shifts of even- and odd-parity wave functions have to be distinguished.

There is another surprising feature of these operators. The number of bound states of the operators which arise in the limits $R \to 0$ and $R \to \infty$ differs from those for finite values of R. This casts some doubts on the usefulness of such operators for an approximation of the products (3.13), (3.14). However, by a careful analysis using the explicit form of Levinson's theorem in 1D, we show that the exact fluctuation determinants converge to those evaluated by means of the limiting operators.

The second method[35] uses the explicit knowledge of the zero mode for the evaluation of the fluctuation determinants. This allows an exact determination of the statistical prefactor for the φ fluctuations. For p fluctuations an analytical treatment is only possible in the limit $Q^{-1} \to 0$.

These results can then be combined to obtain analytical expressions for the total statistical prefactor in the limit of small and large nuclei as well as in the limits $Q^{-1} \to 0$ and $Q^{-1} \to \infty$. In the limit $Q^{-1}\delta^2 \to \infty$ corresponding to either small nuclei or large hard-axis anisotropy, the out-of-easy-plane fluctuations are suppressed and do not contribute at all. While the latter result is to be expected from the fact that out-of-easy-plane fluctuations are suppressed due to their mass Q^{-1}, the former result is somewhat surprising. It is related to the divergence of the characteristic length scale for $R \to 0$ which renders even a small hard-axis anisotropy effectively large. In both limits the system may be described by an effective model discarding the out-of-easy-plane degree of freedom. As we will later address, this model is equivalent to a double sine-Gordon model in the azimuthal variable ϕ.

A. Scattering phase shift method

In this section we evaluate the products (3.13), (3.14) using the knowledge of bound state energies and scattering phase shifts of the operators $\mathcal{H}^{s\varphi}$, $\mathcal{H}^{sp}$ which have been evaluated in paper I.

In order to evaluate the density of states we consider eigenfunctions obeying periodic boundary conditions. The modes around the *metastable* state $(\phi_m, \theta_m) = (\pi, \pi/2)$ are then the plane wave eigenfunctions of the operators (2.23) which can also be written as $\sin kx$, $\cos kx$ with wave numbers

$$k = \frac{2\pi n}{L}, \tag{4.1}$$

where $n = 0, 1, \ldots$ for even-parity and $n = 1, 2, \ldots$ for odd-parity continuum eigenstates. The corresponding density of states is

$$\rho^{mi}_{(j)} = \frac{dn}{dk} = \frac{L}{2\pi}, \qquad i = \varphi, p\,, \quad j = e, o. \tag{4.2}$$

At the *saddle point* $(\phi_s(x), \pi/2)$, however, we encounter a different situation. The nonuniformity of the nucleus, i.e., the nonconstant potentials in $\mathcal{H}^{s\varphi}, \mathcal{H}^{sp}$, lead to phase shifts of the continuum eigenfunctions. In contrast to 3D problems, where the wave function always vanishes at the origin, we have to distinguish between the phase shifts of even- (e) and odd- (o) parity wave functions. We define phase shifts as in paper I,

$$\chi^{si}_{k,(e)}(x \to \pm\infty) \propto \cos[kx \pm \Delta^i_{(e)}(k)/2], \tag{4.3}$$

$$\chi^{si}_{k,(o)}(x \to \pm\infty) \propto \sin[kx \pm \Delta^i_{(o)}(k)/2], \quad i = \varphi, p. \tag{4.4}$$

Since only the eigenfunctions of $\mathcal{H}^{s\,\varphi,p}$ exhibit a phase shift, we have omitted the superscript s on Δ. Note that all phase shifts also depend on the parameter R. Periodic boundary conditions together with (4.3), (4.4) imply

$$kL + \Delta^i_{(j)}(k) = 2\pi n, \quad n = 1, 2, \ldots, \tag{4.5}$$

where $i = \varphi, p$ and $j = e, o$. Following the arguments of Ref. 11, the lowest allowed[36] k values in (4.5) are $k = 2\pi/L$ for odd-parity eigenfunctions and $k = \pi/L$ for even-parity eigenfunctions. Note the surprising fact that the latter value does not coincide with the lowest k value (4.1) of even-parity solutions in the absence of a potential.

The density of states for odd-parity continuum eigenfunctions follows from (4.5),

$$\rho^{si}_{(o)}(k) = \frac{dn}{dk} = \frac{L}{2\pi} + \frac{1}{2\pi}\frac{d\Delta^i_{(o)}(k)}{dk}, \qquad i = \varphi, p. \tag{4.6}$$

Since the spectrum of even-parity continuum eigenfunctions starts at $k = \pi/L$ while free solutions start at $k = 0$, the density of states exhibits an additional δ-function contribution at $k \to 0$,

$$\rho^{si}_{(e)}(k) = \frac{L}{2\pi} + \frac{1}{2\pi}\frac{d\Delta^i_{(e)}(k)}{dk} - \frac{1}{2}\delta(k - 0^+), \quad i = \varphi, p. \tag{4.7}$$

This δ function also ensures that the number of states of the free problem equals that of the scattering problem including bound states,

$$\int_0^\infty dk \left[\rho^{mi}_{(j)} - \rho^{si}_{(j)}(k)\right] = N^i_{(j)}, \quad i = \varphi, p, \quad j = e, o, \tag{4.8}$$

where, according to (6.25) of paper I,

$$N^p_{(e)} = N^p_{(o)} = N^\varphi_{(o)} = 1, \quad N^\varphi_{(e)} = 2 \tag{4.9}$$

are the number of even- and odd-parity bound states of $\mathcal{H}^{s\varphi}$ and $\mathcal{H}^{sp}$. Equation (4.8) with (4.9) is verified using (4.6), (4.7), and 1D Levinson's theorem [(6.23) and 6.24) of paper I] which states that

$$\Delta^p_{(e)}(k=0) = \pi, \quad \Delta^p_{(o)}(k=0) = 2\pi,$$
$$\Delta^\varphi_{(e)}(k=0) = 3\pi, \quad \Delta^\varphi_{(o)}(k=0) = 2\pi. \tag{4.10}$$

We are now in a position to express the ratio of the products in (3.13) in terms of the density of states:

$$\frac{\prod_k E^{mi}_k}{\prod_{k'} E^{si}_{k'}} = \exp\left\{\int_0^\infty dk \left[\rho^{mi}_{(e)} + \rho^{mi}_{(o)} - \rho^{si}_{(e)}(k) - \rho^{si}_{(o)}(k)\right] \times \ln E^{si}_k\right\}, \tag{4.11}$$

where $i = \varphi, p$. After inserting (3.14), (4.6), (4.7) into (4.11), using (4.10), and performing a partial integration we obtain for the φ fluctuations

$$\frac{\prod_k E^{m\varphi}_k}{\prod_{k'} E^{s\varphi}_{k'}} = \delta^{-6} \exp\left\{\int_0^\infty \frac{dk}{\pi}\left[\Delta^\varphi_{(e)} + \Delta^\varphi_{(o)}\right]\frac{k\delta^2}{1 + k^2\delta^2}\right\}, \tag{4.12}$$

where we used the fact that the phase shifts vanish as $1/k\delta$ for $k \to \infty$ according to Born's approximation [(6.29 of paper I)]. In a completely analogous way we obtain for the p fluctuations

$$\frac{\prod_k E^{mp}_k}{\prod_{k'} E^{sp}_{k'}} = \left(Q^{-1} + \delta^{-2}\right)^2 \times \exp\left\{\int_0^\infty \frac{dk}{\pi}\left[\Delta^p_{(e)} + \Delta^p_{(o)}\right] \times \frac{k\delta^2}{1 + Q^{-1}\delta^2 + k^2\delta^2}\right\}. \tag{4.13}$$

Note that in contrast to (4.11), the integrands in (4.12) and (4.13) are independent of the $k \to 0$ limit which due to Levinson's theorem is sensitive to the number of bound states. This fact renders (4.12) and (4.13) suitable for phase shift approximations that converge nonuniformly to the exact phase shifts for $k \to 0$.

In the next two subsections we explicitly evaluate the prefactor in the limit of small and large nuclei. We show that taking the limit $R \to 0, \infty$ of (4.12), (4.13) is equivalent to a direct evaluation of the determinants of the operators that arise in these limits.

1. *Prefactor for $h \to 1$*

In the limit $R \to 0$, when the external field is very close to the anisotropy field, the nucleus represents a slight but spatially extended deviation from the metastable state. The operators $\mathcal{H}^{s\varphi}$ and $\mathcal{H}^{sp}$ given by (2.13) and (2.14) then reduce to

$$\bar{\mathcal{H}}^{s\varphi} = -\frac{d^2}{dx^2} + \delta^{-2}\left(1 - 6\,\mathrm{sech}^2\,\frac{x}{\delta}\right), \tag{4.14}$$

$$\bar{\mathcal{H}}^{sp} = -\frac{d^2}{dx^2} + \delta^{-2}\left(1 - 2\,\mathrm{sech}^2\,\frac{x}{\delta}\right)Q^{-1}. \tag{4.15}$$

The potentials in (4.14), (4.15) are reflectionless and the solution of the corresponding eigenvalue problems is well known (see also the Appendix of paper I). There are bound states with the energies

$$\bar{E}_0^{s\varphi} = -3\delta^{-2}, \quad \bar{E}_1^{s\varphi} = 0,$$
$$\bar{E}_0^{sp} = Q^{-1}. \tag{4.16}$$

Note that the two eigenvalues $E_2^{s\varphi}$, E_1^{sp} of $\mathcal{H}^{s\varphi}$ and $\mathcal{H}^{sp}$ turn into zero energy resonances[37] of $\bar{\mathcal{H}}^{s\varphi}$ and $\bar{\mathcal{H}}^{sp}$ and have therefore no counterparts in (4.16). The continuum eigenvalues of (4.14) and (4.15) are given by (3.15), respectively. Since the potentials are reflectionless, the scattering phase shifts are parity independent and given by

$$\bar{\Delta}^{\varphi}(k) = 2\arctan\frac{3k\delta}{(k\delta)^2 - 2}, \tag{4.17}$$

$$\bar{\Delta}^{p}(k) = 2\arctan\frac{1}{k\delta}, \tag{4.18}$$

and their long-wavelength behavior

$$\bar{\Delta}^{\varphi}(k \to 0) = 2\pi, \quad \bar{\Delta}^{p}(k \to 0) = \pi \tag{4.19}$$

is in accordance with Levinson's theorem [(6.27) of paper I] for *reflectionless* potentials. As has been discussed in paper I, Sec. VIB, the convergence of $\bar{\Delta}^{\varphi}$, $\bar{\Delta}^{p}$ towards the exact phase shifts $\Delta_{(j)}^{si}$ is in general nonuniform for $k = 0$ (cf. Figs. 6,7 of paper I). However, since the integrand in (4.12) and (4.13) vanishes for $k = 0$, we can safely insert the approximations (4.17) and (4.18) into (4.12), (4.13), respectively, and obtain

$$\lim_{R\to 0}\frac{\prod_k E_k^{m\varphi}}{\prod_{k'} E_{k'}^{s\varphi}} = 36\,\delta^{-6} \tag{4.20}$$

and

$$\lim_{R\to 0}\frac{\prod_k E_k^{mp}}{\prod_{k'} E_{k'}^{sp}} = Q^{-2}, \tag{4.21}$$

respectively. For the evaluation of the determinants, we substitute the bound states (4.16) for those in (3.13) and (3.14). However, we have to complete (4.16) by the zero energy resonances $E_2^{s\varphi} = \delta^{-2}$, $E_1^{sp} = Q^{-1} + \delta^{-2}$. Together with (4.20) and (4.21), we then obtain

$$\lim_{R\to 0}\frac{\det\mathcal{H}^{m\varphi}}{\det'|\mathcal{H}^{s\varphi}|} = 12\,\delta^{-2} \tag{4.22}$$

and

$$\lim_{R\to 0}\frac{\det\mathcal{H}^{mp}}{\det\mathcal{H}^{sp}} = 1, \tag{4.23}$$

where in (4.20), (4.22), $\delta^{-2} = R^2$. The result (4.23) is remarkable since it shows that the fluctuations in the p-direction do not play a role at all for small nuclei, independent of the size of the hard-axis anisotropy constant. This suggests that in the limit $R \to 0$ the system may effectively be described by a double sine-Gordon equation in the azimuthal angle ϕ. We shall return to this issue in Sec. VII.

Alternatively, although less carefully, we can interchange the limit $R \to 0$ with the functional integration, and directly calculate

$$\frac{\det\mathcal{H}^{m\varphi}}{\det'|\bar{\mathcal{H}}^{s\varphi}|} = \frac{\prod_k E_k^{m\varphi}}{|\bar{E}_0^{s\varphi}|\prod_{k'}\bar{E}_{k'}^{s\varphi}},$$
$$\frac{\det\mathcal{H}^{mp}}{\det\bar{\mathcal{H}}^{sp}} = \frac{\prod_k E_k^{mp}}{\bar{E}_0^{sp}\prod_{k'}\bar{E}_{k'}^{sp}}. \tag{4.24}$$

For the evaluation of the rhs in (4.24) we proceed similarly to the derivation of (4.12) and (4.13) with the following modifications: The density of states $\rho_{(j)}^{mi} - \rho_{(j)}^{si}(k)$ in (4.11) has to be replaced by $\bar{\rho}_{(j)}^{mi} - \bar{\rho}_{(j)}^{si}(k) = -\frac{1}{2\pi}d\bar{\Delta}^i/dk$ with $\bar{\Delta}^i$ given by (4.17) and (4.18) ($i = \varphi, p$). Using the version (4.19) of Levinson's theorem together with (4.17) and (4.18), we recover the results (4.22) and (4.23) after integration.

To summarize, we thus have shown that the small nucleus approximation may be used for the evaluation of the fluctuation determinants, or explicitly

$$\lim_{R\to 0}\frac{\det\mathcal{H}^{m\varphi}}{\det'|\mathcal{H}^{s\varphi}|} = \frac{\det\mathcal{H}^{m\varphi}}{\det'|\bar{\mathcal{H}}^{s\varphi}|},$$
$$\lim_{R\to 0}\frac{\det\mathcal{H}^{mp}}{\det\mathcal{H}^{sp}} = \frac{\det\mathcal{H}^{mp}}{\det\bar{\mathcal{H}}^{sp}}, \tag{4.25}$$

where the rhs has been evaluated in leading order in R. The relation (4.25) has not been clear on the onset, since the operators $\bar{\mathcal{H}}^{s\varphi}$, $\bar{\mathcal{H}}^{sp}$ exhibit a different number of bound states and different long-wavelength behavior of the scattering phase shifts than the operators $\mathcal{H}^{s\varphi}$, $\mathcal{H}^{sp}$. As we have shown now, these two differences conspire in such a way that an interchange of the limits in (4.25) is indeed correct.

2. *Prefactor for $h \to 0$*

For $R \gg 1$ the nucleus separates into two independent π-Bloch walls. Correspondingly $\mathcal{H}^{s\varphi}$ and $\mathcal{H}^{sp}$ merge into the same operator $\hat{\mathcal{H}}^{s}$ which consists of two independent potential wells of the form $-2\delta^{-2}\,\mathrm{sech}^2(x/\delta \pm R)$. The bound states of $\hat{\mathcal{H}}^{s}$ are then given by the symmetric and antisymmetric linear combinations of the ground states of the single wells and have energies [cf. (6.4) and (6.6) of paper I)]

$$\hat{E}_0^{sp} = Q^{-1}, \quad \hat{E}_1^{sp} = Q^{-1} + 8e^{-2R},$$
$$\hat{E}_0^{s\varphi} = -8e^{-2R}, \quad \hat{E}_1^{s\varphi} = 0. \tag{4.26}$$

Note that in this approximation $E_2^{s\varphi}$ has merged into a zero energy resonance of $\hat{\mathcal{H}}^{s}$. The continuum eigenvalues

are identical to (3.15) while the scattering phase shifts are twice those of a single potential well [cf. (6.18)],

$$\hat{\Delta}^s(k) = 4 \arctan \frac{1}{k\delta}. \tag{4.27}$$

The coincidence of the phase shifts of even and odd eigenfunctions originates from the fact that the two $-2\,\mathrm{sech}^2 x$ potential wells are reflectionless. The phase shifts (4.27) obey the reflectionless version of Levinson's theorem, i.e., $\hat{\Delta}^s(k \to 0) = \pi N$ with N the number of bound states. But as in the previous subsection, the phase shifts $\Delta^{s\varphi}_{(e)}$ and $\Delta^{sp}_{(e)}$ only converge on the open interval $0 < k < \infty$ towards $\hat{\Delta}^s$. Inserting (4.27) into (4.12), (4.13), and using (4.26) together with $E_2^{s\varphi} = \delta^{-2}$ in (3.13), (3.14), we obtain

$$\lim_{R\to\infty} \frac{\det \mathcal{H}^{m\varphi}}{\det' |\mathcal{H}^{s\varphi}|} = 2\, e^{2R}, \tag{4.28}$$

$$\lim_{R\to\infty} \frac{\det \mathcal{H}^{mp}}{\det \mathcal{H}^{sp}} = [\sqrt{1+Q} + \sqrt{Q}]^4. \tag{4.29}$$

The latter result approaches 1 for large hard-axis anisotropies as expected. However, in the opposite limit of high Q, the p fluctuations lead to a prefactor (3.12) proportional to Q.

3. *Out-of-easy-plane fluctuations for $Q^{-1}\delta^2 \to \infty$*

A large hard-axis anisotropy leads to the suppression of out-of-easy-plane fluctuations by the existence of a large mass gap. Therefore we expect the fluctuation determinant to become one in this limit.

To prove this conjecture, we remark that $\Delta^{sp}_{(e)}$, $\Delta^{sp}_{(o)}$ are continuous functions which are proportional to $1/k\delta$ for $k \to \infty$ according to Born's approximation [(6.29 of paper I)] and remain finite for $k \to 0$ due to Levinson's theorem. Therefore both phase shifts obey the inequality $\Delta(k) < c/k\delta$ with a suitably chosen constant c. For the integral in (4.13) we thus obtain the inequality

$$0 < \int_0^\infty \frac{dk}{\pi} \frac{k\delta^2 \left[\Delta^p_{(e)} + \Delta^p_{(o)}\right]}{1 + Q^{-1}\delta^2 + k^2\delta^2} < \frac{d}{\sqrt{1+Q^{-1}\delta^2}}, \tag{4.30}$$

where $d = (c^p_{(e)} + c^p_{(o)})/2$. Since d is independent of Q, the upper limit tends to zero for $Q^{-1}\delta^2 \to \infty$ and therefore we have with $E_0^{sp} \equiv Q^{-1}$, $E_1^{sp} = Q^{-1} + \varepsilon\delta^{-2}$ with $0 < \varepsilon < 1$ and (4.13), (3.14),

$$\lim_{Q^{-1}\delta^2\to\infty} \frac{\det \mathcal{H}^{mp}}{\det \mathcal{H}^{sp}} = 1. \tag{4.31}$$

In fact we have now shed some new light on the result (4.23). The hard-axis anisotropy does not enter (4.30) in isolated form but rather in the combination $Q^{-1}\delta^2 = Q^{-1}\coth^2 R$ which shows that due to the diverging length scale, the hard-axis anisotropy becomes effectively strong for small R, no matter how small Q^{-1} is.

B. Jacobi method

There is also an alternative way for evaluating the products of eigenvalues which has its origin in the space slice representation of the path integrals. This method allows for the exact evaluation of the statistical prefactor in the φ variable for all values of R. In the limit $Q^{-1} = 0$ we are also able to evaluate the prefactor for out-of-easy-plane fluctuations. We first show how this method can be applied to the evaluation of (3.13). According to Ref. 34 we have

$$\frac{\det_L \mathcal{H}^{m\varphi}}{\det_L \mathcal{H}^{s\varphi}} = \frac{D^{(0)}_\varphi(L/2)}{D_\varphi(L/2)}. \tag{4.32}$$

The notation $\det_L$ on the lhs of (4.32) indicates that the evaluation of the determinants relies on eigenvalue problems defined on the finite interval $[-L/2, L/2]$ with respect to functions that vanish at the end of the interval. The functions D_φ and $D^{(0)}_\varphi$ on the rhs of (4.32) are solutions of the differential equations

$$\mathcal{H}^{s\varphi} D_\varphi(x) = 0, \tag{4.33}$$

$$\left(-\frac{d^2}{dx^2} + \delta^{-2}\right) D^{(0)}_\varphi(x) = 0, \tag{4.34}$$

with the "initial" conditions (the prime denotes d/dx)

$$D_\varphi(-L/2) = 0, \quad D'_\varphi(-L/2) = 1\,, \tag{4.35}$$

$$D^{(0)}_\varphi(-L/2) = 0, \quad D^{(0)\prime}_\varphi(-L/2) = 1. \tag{4.36}$$

Note that on the finite interval the first excited eigenfunction of $\mathcal{H}^{s\varphi}$ has no longer zero energy and therefore the lhs of (4.32) is well defined. The eigenvalue problem of this quasi-zero-energy mode is written as

$$\mathcal{H}^{s\varphi} f = \mu f, \tag{4.37}$$

where for large system lengths L, $\mu > 0$ is small, and f obeys the boundary conditions $f(\pm L/2) = f'(\pm L/2) = 0$. Note that for $L \to \infty$ we have $f \to \chi_1^{s\varphi}$ and $\mu \to 0$. The fluctuation determinant is then obtained as follows:

$$\frac{\det \mathcal{H}^{m\varphi}}{\det' |\mathcal{H}^{s\varphi}|} = \lim_{L\to\infty} \left| \mu\, \frac{D^{(0)}_\varphi(L/2)}{D_\varphi(L/2)} \right|. \tag{4.38}$$

We now turn to the evaluation of the rhs of (4.38). $D^{(0)}_\varphi(L/2)$ is easily obtained by integration of (4.34) with (4.36),

$$D^{(0)}_\varphi(L/2) = \delta \sinh(L/\delta) \simeq \frac{\delta}{2} e^{L/\delta}. \tag{4.39}$$

The function $D_\varphi(x)$ obeys the same differential equation (4.33) as the zero mode $\chi_1^{s\varphi}(x)$ (2.20), but subject to different boundary conditions (4.35). Therefore $D_\varphi(x)$ is a linear combination of $\chi_1^{s\varphi}(x)$ and the unknown linear independent solution $\xi_1^{s\varphi}(x)$ of the differential equation (4.33),

$$D_\varphi(x) = u\chi_1^{s\varphi}(x) + v\xi_1^{s\varphi}(x), \tag{4.40}$$

with real constants u, v. $\chi_1^{s\varphi}$ is taken to be unnormalized,

$$\chi_1^{s\varphi} = \frac{d\phi_s}{dx} = \delta^{-1}\left[\operatorname{sech}(x/\delta - R) - \operatorname{sech}(x/\delta + R)\right]. \tag{4.41}$$

The normalization of $\xi_1^{s\varphi}(x)$ is chosen such that the Wronskian

$$\chi_1^{s\varphi}\frac{\partial \xi_1^{s\varphi}}{\partial x} - \xi_1^{s\varphi}\frac{\partial \chi_1^{s\varphi}}{\partial x} = 1. \tag{4.42}$$

In order to satisfy the initial conditions (4.35), we must have

$$u = -\xi_1^{s\varphi}(-L/2), \qquad v = \chi_1^{s\varphi}(-L/2). \tag{4.43}$$

From (4.41) we infer the asymptotic behavior

$$\chi_1^{s\varphi} \to N\operatorname{sgn}(x)e^{-|x|/\delta} \quad \text{for } x \to \pm\infty, \tag{4.44}$$

with

$$N = 4\delta^{-1}\sinh R. \tag{4.45}$$

The symmetry of the potential in $\mathcal{H}^{s\varphi}$ and the antisymmetry of $\chi_1^{s\varphi}$ allow us to choose $\xi_1^{s\varphi}$ as a symmetric function which has the asymptotic behavior,

$$\xi_1^{s\varphi} \to N' e^{|x|/\delta}, \quad \text{for } x \to \pm\infty. \tag{4.46}$$

From (4.42) it follows that

$$N' = \frac{\delta}{2N}, \tag{4.47}$$

and therefore with (4.43)–(4.47) we have

$$D_\varphi(L/2) = -\delta. \tag{4.48}$$

Finally we are left with the evaluation of μ. The eigenfunction f may to first order in μ be expressed as

$$f(x) = \eta(x) + \mu\int_{-L/2}^{L/2} G(x,y)\eta(y)dy, \tag{4.49}$$

with the Green's function

$$G(x,y) = \theta(x-y)[\chi_1^{s\varphi}(x)\xi_1^{s\varphi}(y) - \chi_1^{s\varphi}(y)\xi_1^{s\varphi}(x)]. \tag{4.50}$$

The quasi-zero-energy eigenvalue μ is now determined such that $f(\pm L/2) = 0$. The function η is a solution of the homogeneous problem (4.33) which satisfies the boundary condition $\eta(-L/2) = 0$,

$$\eta(x) = \chi_1^{s\varphi}(x) + c\xi_1^{s\varphi}(x), \tag{4.51}$$

with

$$c = -\chi_1^{s\varphi}(-L/2)/\xi_1^{s\varphi}(-L/2). \tag{4.52}$$

The requirement $f(L/2) = 0$ then leads to

$$\mu = \frac{\chi_1^{s\varphi}(L/2) + c\xi_1^{s\varphi}(L/2)}{\int_{-L/2}^{L/2} dy\{[\chi_1^{s\varphi}(y)]^2\xi_1^{s\varphi}(L/2) - c\chi_1^{s\varphi}(L/2)[\xi_1^{s\varphi}(y)]^2\}}. \tag{4.53}$$

Since the normalization of $\chi_1^{s\varphi}$ is independent of L, the first term in the denominator is of the order $\exp(L/2\delta)$ whereas the second vanishes as $\exp(-L/2\delta)$ and thus may be neglected. In leading order in $\exp(-L/\delta)$ we thus obtain

$$\mu = \frac{2\chi_1(L/2)}{\xi_1(L/2)\int_{-L/2}^{L/2}\chi_1^2(y)} = \frac{64\,\delta^{-3}\sinh^2 R}{\mathcal{E}_s(R)}e^{-L/\delta}, \tag{4.54}$$

where we have made use of (4.41) of this paper and (3.12) of paper I. Inserting (4.39), (4.48), and (4.54) into (4.38) and performing the limit $L \to \infty$, we finally obtain the result

$$\frac{\det \mathcal{H}^{m\varphi}}{\det'|\mathcal{H}^{s\varphi}|} = \frac{8\tanh^3 R\sinh^2 R}{\tanh R - R\operatorname{sech}^2 R}, \tag{4.55}$$

which is *exact* for all values of the external field. Note that in the limits $R \to 0$ and $R \to \infty$, Eq. (4.55) reduces to the results (4.22), (4.28), respectively.

The above method cannot be used for the evaluation of the p determinants (4.58) for arbitrary values of the hard-axis anisotropy since the zero energy eigenfunction of $\mathcal{H}^{sp}$ is not explicitly known. In the limit of small $Q^{-1}\delta^2$, however, the fluctuation determinant may be calculated exactly.

The Q^{-1}-independent operator $\mathcal{H}^{sp} - Q^{-1}$ exhibits the zero energy mode χ_0^{sp} and we can proceed along the same lines[40] as in the derivation of (4.55) to obtain

$$\frac{\det(\mathcal{H}^{mp} - Q^{-1})}{\det'(\mathcal{H}^{sp} - Q^{-1})} = \frac{8\tanh^3 R\cosh^2 R}{\tanh R + R\operatorname{sech}^2 R}, \tag{4.56}$$

where the prime denotes omission of the zero energy mode. From (4.11) with (3.15) it follows that $\prod_k E_k^{mp}/\prod_k' E_k'^{sp} = \prod_k(E_k^{mp} - Q^{-1})/\prod_k'(E_k'^{sp} - Q^{-1}) + \mathcal{O}(Q^{-1}\delta^2)$. With (3.14) we then obtain in leading order in the small parameter $Q^{-1}\delta^2$

$$\begin{aligned}\frac{\det \mathcal{H}^{mp}}{\det \mathcal{H}^{sp}} &= \frac{1}{E_0^{sp}}\frac{E_1^{sp} - Q^{-1}}{E_1^{sp}}\frac{\det(\mathcal{H}^{mp} - Q^{-1})}{\det'(\mathcal{H}^{sp} - Q^{-1})} \\ &= Q\frac{E_1^{sp} - Q^{-1}}{E_1^{sp}}\frac{8\tanh^3 R\cosh^2 R}{\tanh R + R\operatorname{sech}^2 R}.\end{aligned} \tag{4.57}$$

The second factor on the rhs has been retained since the coefficients of its power expansion in $Q^{-1}\delta^2$ diverge for $R \to \infty$. However, in the limit $Q^{-1} \ll E_1^{sp}$ (R not too large), it reduces to 1. Note that the result (4.57) is only valid for $Q^{-1}\delta^2$ small and it can therefore not be used for R small. In this latter case (4.31) applies.

With the exact result (4.55), the prefactor (3.12) now takes the form

$$\Omega = \lambda_+ L\sqrt{\beta\mathcal{A}}\frac{4}{\pi^{3/2}}\tanh^{3/2} R\,\sinh R\sqrt{\frac{\det \mathcal{H}^{mp}}{\det \mathcal{H}^{sp}}}, \tag{4.58}$$

which is further evaluated in the following section.

V. NUCLEATION RATES IN THE OVERDAMPED LIMIT

In this section we shall derive analytical results for the prefactor (4.58) in the limit of large and small values of $Q^{-1}\delta^2$ as well as large R. In the intermediate parameter range the prefactor is evaluated numerically. The discussion in this section is restricted to the regime of large damping. The case of moderate damping which is more relevant for real systems shall be discussed in the next section.

We start with the evaluation of the decay frequency λ_+ of the nucleus. For large values of the damping constant α, the Eqs. (3.2) characterizing the unstable mode of the nucleus decouple and take the form

$$\begin{aligned}\lambda_+\varphi_+ &= -\alpha\mathcal{H}^{s\varphi}\varphi_+,\\ \lambda_+ p_+ &= -\alpha\mathcal{H}^{sp}p_+,\end{aligned} \tag{5.1}$$

with $\lambda_+ > 0$. The unstable mode is thus given by the ground state of $\mathcal{H}^{s\varphi}$, i.e., $(\varphi_+, p_+) \propto (\chi_0^{s\varphi}, 0)$, and for large α the corresponding escape frequency is given by

$$\lambda_+ = \alpha|E_0^{s\varphi}(R)|. \tag{5.2}$$

The eigenvalue $E_0^{s\varphi}(R)$ has been investigated in paper I. It is known analytically in the limits $R \to 0, \infty$ [cf. (4.16), (4.26), respectively] which allows an explicit evaluation of the prefactor in these limits.

(i) For large nuclei ($R \to \infty$) we may use (4.26), (4.29), and together with $\mathcal{E}_s \to 4$ and the prefactor (4.58) takes the form

$$\Omega = \alpha L\sqrt{\beta\mathcal{A}}\frac{16}{\pi^{3/2}}\left[\sqrt{Q} + \sqrt{1+Q}\right]^2 e^{-R}. \tag{5.3}$$

(ii) For $Q^{-1}\delta^2 \gg 1$, (4.31) and (5.2) may be inserted into (4.58) to yield

$$\Omega = \alpha L\sqrt{\beta\mathcal{A}}\frac{4}{\pi^{3/2}}|E_0^{s\varphi}(R)|\tanh^{3/2}R\,\sinh R. \tag{5.4}$$

For small R, this reduces to

$$\Omega = \alpha L\sqrt{\beta\mathcal{A}}\frac{12}{\pi^{3/2}}R^{9/2}. \tag{5.5}$$

Note that the results (5.4) and (5.5) are both independent of the value of the hard-axis anisotropy.

(iii) In the limit $Q^{-1}\delta^2 \to 0$ we can use (4.58) and (4.57) to obtain

$$\Omega = \alpha L\sqrt{\beta\mathcal{A}}\frac{8\sqrt{2}}{\pi^{3/2}}|E_0^{s\varphi}|\sqrt{Q}\sqrt{\frac{E_1^{sp}-Q^{-1}}{E_1^{sp}}} \times\frac{\tanh^2 R\sinh^2 R}{\sqrt{\tanh R + R\,\mathrm{sech}^2 R}}. \tag{5.6}$$

For values of R such that $Q^{-1} \ll E_1^{sp}(R)$, the square root containing E_1^{sp} reduces to 1. In the limit $R \to \infty$, Eq. (5.6) reduces to (5.3) with $Q^{-1} \to 0$.

Note, however, that the present theory is only valid for hard-axis anisotropies which are not too small such that the amplitude of out-of-easy-plane fluctuations is much smaller than 1. Requiring the thermal expectation value $\langle p^2\rangle$ with respect to the Boltzmann weight $\exp\{-\beta\mathcal{A}\mathcal{E}_s^{(2)}\}$ with $\mathcal{E}_s^{(2)}$ as in (2.12) to be smaller than 1 and noting that the lowest eigenvalue in the p direction is $E_0^{sp} = Q^{-1}$, we obtain for the validity of the present theory the condition $\beta\mathcal{A}\sqrt{AK_e}K_h/K_e > 1$.

For all other parameter values the prefactor has been evaluated numerically. The corresponding results are shown in Fig. 3 with the dashed and dot-dashed lines representing the asymptotic formulas (5.3) and (5.5), respectively. Reinstating the units (2.4) we recognize that the prefactor (3.12) is inversely proportional to α, a fact which is in accordance with the general behavior[16] of nucleation rates in the overdamped limit.

VI. NUCLEATION RATE FOR MODERATE DAMPING

In the last section we have presented results for nucleation rates of thermally activated magnetization reversal in the overdamped limit. In that case, the decay of the nucleus is governed by purely dissipative mechanisms. However, in ferromagnetic materials the damping constant is usually of the order $\alpha = 10^{-2}$ or sometimes as small as 10^{-4} in some high purity materials such as YIG.

According to (3.12), the dynamic properties of the system enter the nucleation rate only[41] in the form of the decay frequency of the nucleus. In order to evaluate the nucleation rate in the moderately damped regime we therefore have to include the conservative, precessional part of the dynamics for the evaluation of the decay frequency λ_+. In the limits of small and large nuclei this decay frequency can again be expressed in closed analytical form, thus enabling us to give exact results of the total prefactor and hence of the total rate. To the best of my knowledge, this provides the first application of

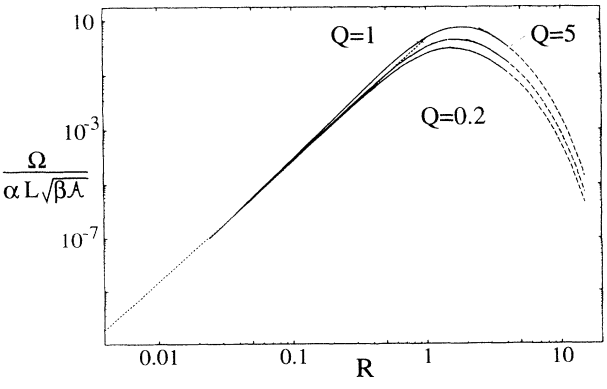

FIG. 3. The reduced prefactor in the overdamped limit is shown as a function of the parameter R for different values of the hard-axis anisotropy. The dot-dashed and dashed lines are the asymptotic formulas (5.5) and (5.3), respectively.

Langer's general theory[7] of moderate friction to a system with infinitely many degree of freedoms.

In a first part we discuss the escape frequency λ_+. We obtain exact expressions in the limits $R \to \infty$ and $Q^{-1}\delta^2 \to \infty$ as well as an approximate formula which expresses λ_+ by $E_0^{s\varphi}$. These results allow an exact evaluation of the nucleation rate in the limits $R \to 0$ and $R \to \infty$.

A. Escape frequency

The dynamically unstable mode (φ_+, p_+) of the nucleus is the solution of the (non-Hermitian) coupled eigenvalue problem (3.2). Before turning to a quantitative analysis we give a qualitative discussion of the parity and relative sign of the functions φ_+, p_+. Both functions are nodeless and symmetric in x with opposite relative sign as may be seen from the following plausibility arguments: For $\alpha \to \infty$ we know from (5.1) that the dynamical unstable mode coincides with the ground state of $\mathcal{H}^{s\varphi}$, i.e., $(\varphi_+, p_+) \propto (\chi_0^{s\varphi}, 0)$, and therefore φ_+ is a symmetric nodeless function in x. For finite values of α there will be a nonzero p_+ component. Since the nucleus represents an untwisted π-Bloch wall pair [cf. (3.11 of paper I)], the instability represents a confluence or a separation of the two domain walls which is associated with a monotonical increase or decrease of the angle ϕ. Hence φ_+ is a symmetric nodeless function in x. To comment on p_+, we have to recall that a motion of the domain wall is only possible if the structure exhibits an out-of-easy-plane component.[45] In order for the domain walls to move in opposite directions, the out-of-easy-plane component must have the same sign at the center of the two oppositely twisted kinks and due to the gyroscopic nature of the equations of motion, p_+ and φ_+ must have opposite signs.

Therefore we are looking for even-parity nodeless solutions of (3.2) with opposite signs. The ambiguity in the overall sign of (φ_+, p_+) describes the freedom of the nucleus either to collapse or to expand. Inspecting (3.2) we recognize that the eigenvalue problem can be easily solved if φ_+ and p_+ are the ground states of $\mathcal{H}^{s\varphi}$ and $\mathcal{H}^{sp}$, respectively, and proportional to each other. This is fulfilled in two limiting cases, (i) R large and (ii) $Q^{-1}\delta^2 \gg 1$.

(i) For large R we have according to (2.19) of this paper and (6.2) of paper I

$$\chi_0^{s\varphi} \propto \chi_0^{sp} \propto \operatorname{sech}(x/\delta + R) + \operatorname{sech}(x/\delta - R). \tag{6.1}$$

Inserting $\varphi_+ \propto p_+ \propto \chi_0^{s\varphi}$ into (3.2) and using that the ground state energy of $\mathcal{H}^{sp}$ is given by $E_0^{sp} \equiv Q^{-1}$ we obtain

$$\lambda_+ = -\frac{\alpha}{2}[Q^{-1} + E_0^{s\varphi}] + \sqrt{\left(\frac{\alpha}{2}\right)^2 [Q^{-1} - E_0^{s\varphi}]^2 - Q^{-1}E_0^{s\varphi}}, \tag{6.2}$$

where $E_0^{s\varphi} \simeq -8e^{-2R}$ in the limit $R \to \infty$. The square root in (6.2) has been retained because the relative magnitude of the (small) parameters $E_0^{s\varphi}$, α, and Q^{-1} has not been specified yet. The corresponding unstable mode is given by

$$(\varphi_+, p_+) \propto \left[\operatorname{sech}\left(\frac{x}{\delta} + R\right) + \operatorname{sech}\left(\frac{x}{\delta} - R\right)\right] \times (1, -Q[\lambda_+ + \alpha E_0^{s\varphi}]). \tag{6.3}$$

The plus sign of the square rooot is chosen in order to reproduce the correct asymptotic behavior (5.2) for large α. Note that Eq. (6.3) agrees with the statements made above: The functions p_+, φ_+ are symmetric and nodeless while the ratio p_+/φ_+ is always negative and vanishes for $\alpha \to \infty$. For $\alpha \to 0$ we have $p_+/\varphi_+ = -\sqrt{Q|E_0^{s\varphi}(R)|}$.

(ii) For $Q^{-1}\delta^2 \gg 1$ we have $\mathcal{H}^{sp}p_+ = Q^{-1}p_+ + \mathcal{O}(\delta^{-2})$. Thus the first equation of (3.2) can be solved for p_+ and after insertion into the second equation of (3.2), the following eigenvalue problem is obtained:

$$\mathcal{H}^{s\varphi}\varphi_+ = -\lambda_+ \frac{\lambda_+ Q + \alpha}{1 + \alpha^2 + \alpha\lambda_+ Q}\,\varphi_+. \tag{6.4}$$

The solution of this equation is known, i.e., $\varphi_+ \propto \chi_0^{s\varphi}$, and hence the coefficient of φ_+ on the rhs equals $E_0^{s\varphi}$. Solving for λ_+ we recover the expressions (6.2) for λ_+ and (6.3) for p_+/φ_+ but with $E_0^{s\varphi}(R)$ now evaluated for arbitrary values of R. This is a remarkable result as it demonstrates the validity of (6.2), (6.3) in the opposite limits $Q^{-1}\delta^2 \gg 1$, $R \gg 1$. Note that for large Q^{-1}, (6.2) and (6.3) hold for all values of R. In the particular case of small R ($\delta^2 \gg 1$) we can insert the small R approximation $E^{s\varphi} = -3R^2 + \mathcal{O}(R^4)$ into (6.2) to obtain

$$\lambda_+ = -\frac{\alpha}{2}[Q^{-1} - 3R^2] + \sqrt{\left(\frac{\alpha}{2}\right)^2 [Q^{-2} + 6Q^{-1}R^2] + 3Q^{-1}R^2}. \tag{6.5}$$

The unstable mode is then given by

$$(\varphi_+, p_+) \propto \operatorname{sech}^2\left(\frac{x}{\delta}\right)(1, -Q(\lambda_+ - 3\alpha R^2)). \tag{6.6}$$

The validity of the expression (6.2) in the opposite limits $R \to 0, \infty$ might hint to a more extended validity. In order to investigate λ_+ for intermediate values of R at arbitrary Q^{-1} we have to resort to numerical methods. It turns out that the direct integration of (3.2) yields rather inaccurate results (errors of 10%). Considerable improvement has been achieved by converting (3.2) into two decoupled fourth-order differential equations in each of the variables φ_+, p_+. As is seen from Fig. 4, Eq. (6.2) provides an excellent approximation to these numerical results.

B. Nucleation rates

We are now in a position to give the results for the prefactor for moderate damping. Results in closed form are obtained in the limits $R \to 0$ and $R \to \infty$. For $Q^{-1}\delta^2 \to \infty$ the prefactor can be expressed in terms of the negative eigenvalue $E_0^{s\varphi}$ which for arbitrary values of

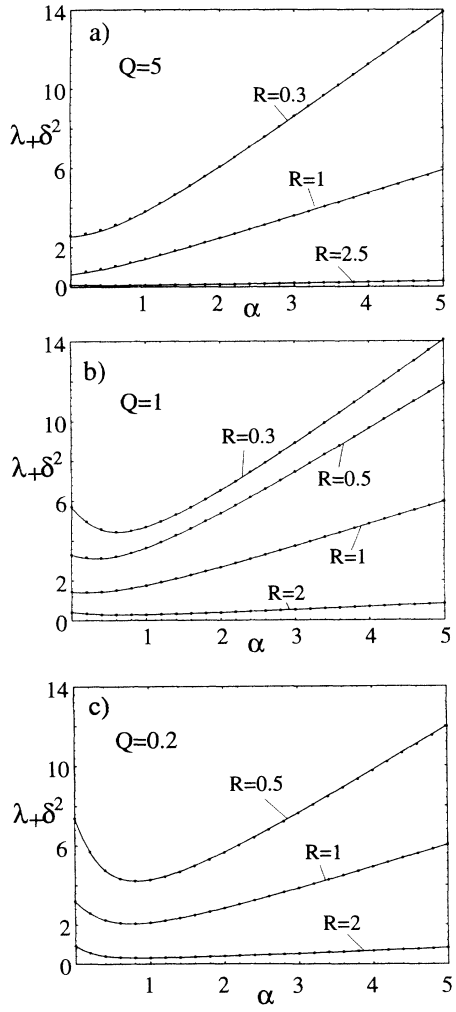

FIG. 4. The decay frequency of the nucleus is shown for different values of R and α. The dots are results of a numerical solution of (3.2) and the solid line is the approximation formula (6.2).

R has to be evaluated numerically.

(i) For large R, we can combine (4.29), (4.58), and (6.2) with $E_0^{s\varphi} = -8e^{-2R}$ to obtain

$$\Omega = L\sqrt{\beta\mathcal{A}}\frac{2}{\pi^{3/2}}[\sqrt{Q}+\sqrt{1+Q}]^2 e^R \times\left\{-\frac{\alpha}{2}(Q^{-1}-8e^{-2R}) +\sqrt{\left(\frac{\alpha^2}{2}\right)[Q^{-2}+16Q^{-1}e^{-2R}]+8Q^{-1}e^{-2R}}\right\}. \tag{6.7}$$

The square root has been retained since the relative order of the small parameters α and e^{-2R} has not been specified yet. However, in an expansion of the square root only leading terms in e^{-2R} should be taken into account.

(ii) For $Q^{-1}\delta^2 \to \infty$, the results (4.58) and (4.31) yield

$$\Omega = \lambda_+ L\sqrt{\beta\mathcal{A}}\frac{4}{\pi^{3/2}}\tanh^{3/2}R\,\sinh R\,, \tag{6.8}$$

with λ_+ given by (6.2). For small R, this result reduces with (6.5) to

$$\Omega = L\sqrt{\beta\mathcal{A}}\frac{4}{\pi^{3/2}}R^{5/2}\left\{-\alpha(Q^{-1}-3R^2) +\sqrt{\left(\frac{\alpha}{2}\right)^2[Q^{-2}+6Q^{-1}R^2]+3Q^{-1}R^2}\right\}. \tag{6.9}$$

Also here, the square root has been retained since we did not specify the relative magnitude of the small parameters α and R. However, we have to keep in mind that upon expansion of the square root only terms in leading order in R have to be kept in order to be consistent with the derivation of the determinant of p fluctuations. For small damping constants $\alpha \ll \sqrt{Q}R$, Eq. (6.9) reduces to

$$\Omega = L\sqrt{\beta\mathcal{A}}\frac{4\sqrt{3}}{\pi^{3/2}}\sqrt{Q^{-1}}R^{7/2}. \tag{6.10}$$

This limit is realized in typical experimental situations.

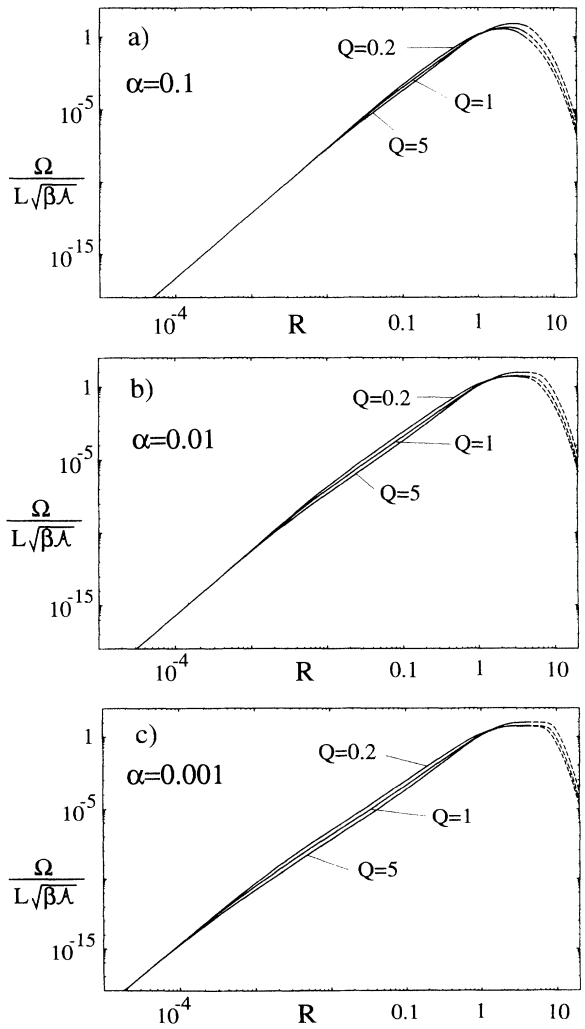

FIG. 5. Numerical results for the reduced prefactor (4.58) for moderate damping as a function of R. The dashed lines represent the asymptotic formula (6.7).

For $\sqrt{Q}R \ll \alpha$ we obtain

$$\Omega = L\sqrt{\beta\mathcal{A}}\frac{12}{\pi^{3/2}}\left(\alpha+\frac{1}{\alpha}\right)R^{9/2}. \tag{6.11}$$

For large values of α, Eq. (6.11) merges into the prefactor for the overdamped regime (5.5).

The above results for the prefactor are summarized in Table I. In Fig. 5, numerical results for the prefactor are shown for arbitrary values of R. The prefactor is maximal for $R \simeq 1$ and decreases as the external field approaches the anisotropy field, i.e., $h \to 1$, or as the field approaches zero. One clearly recognizes that Ω is independent of the hard-axis anisotropy Q^{-1} and the damping constant α for small and intermediate values of R, respectively, as predicted by (6.11), (6.10).

The total rate for magnetization reversal is then given by (3.11) and experimental consequences of this result shall be discussed in Sec. VIII. A detailed discussion of experimental implications of these results may also be found in Ref. 42.

VII. RELATION TO THE DOUBLE SINE-GORDON SYSTEM

In this section it is shown that the results of the previous sections allow us to calculate the nucleation rate of kink-antikink pairs of the double sine-Gordon model for moderate to large friction. Second, we shall see that in the limit $Q^{-1}\delta^2 \to \infty$ (i.e., large hard-axis anisotropy and/or fields close to the anisotropy field), magnetization reversal rates become equivalent to the creation rates of kink-antikink pairs in the double sine-Gordon model.

Discarding noise terms for the moment, we consider the dynamics of a field variable $\phi(x,t)$ which is governed by the damped double sine-Gordon equation

$$Q\partial_t^2\phi + \alpha\partial_t\phi = -\frac{\delta\mathcal{E}_{\rm dSG}}{\delta\phi}, \tag{7.1}$$

with the energy

$$\mathcal{E}_{\rm dSG} = \int_{L/2}^{L/2} dx\left\{\frac{1}{2}(\partial_x\phi)^2 + \frac{1}{2}\sin^2\phi - h\cos\phi\right\}. \tag{7.2}$$

The constant Q plays the role of a mass and α is a damping constant. In the overdamped limit, the inertia term $Q\partial_t^2\phi$ in (7.1) can be neglected and the dynamics is purely determined by the damping term. Note that (7.2) is equivalent to the energy density (2.5) restricted to the easy plane $\theta = \pi/2$. Therefore, Eq. (7.1) exhibits the same saddle point solution ϕ_s [Eq. (2.9)] as the full magnetic system. The corresponding barrier energy between the metastable state $\phi = \pi$ and the absolute minimum $\phi = 0$ is given by $\mathcal{E}_s$ [Eq. (2.15)]. Expanding $\phi(x,t) = \phi_s(x) + \varphi(x,t)$ and linearizing the equation of motion (7.1) around the saddle point yields

$$Q\partial_t^2\varphi + \alpha\partial_t\varphi + \mathcal{H}^{s\varphi}\varphi = 0, \tag{7.3}$$

where $\mathcal{H}^{s\varphi}$ is given by (2.13). A description of the stochastic dynamics in the vicinity of the saddle is obtained by adding the stochastic force $\xi(x,t)$ to the rhs of (7.3) with the noise correlation $\langle\xi(x',t')\xi(x,t)\rangle = (2\alpha/\tilde{\beta})\delta(x-x')\delta(t-t')$. The corresponding Fokker-Planck equation takes the form of (3.8) if we identify $\tilde{\beta} = \beta\mathcal{A}$, $M_{11} = 0$, $M_{12} = -M_{21} = 1$, $M_{22} = \alpha$, and $\mathcal{H} = (\mathcal{H}^{s\varphi}, Q^{-1})$.

TABLE I. Summary of the results for the prefactor Ω [Eq. (4.58)] in the moderately damped limit for (i) large effective hard-axis anisotropy $Q^{-1}\delta \gg 1$, ($\delta = \coth R$), and (ii) small fields $R \gg 1$ ($h = \mathrm{sech}^2 R$). Note that the underlying dimensionless units are given by (2.4).

	$\Omega/L\sqrt{\beta\mathcal{A}}$	λ_+	$E_0^{s\varphi}$
(i) $Q^{-1}\delta^2 \gg 1$[a]	$\frac{4\lambda_+}{\pi^{3/2}}\tanh^{3/2}R\sinh R$	$-\frac{\alpha}{2}[Q^{-1}+E_0^{s\varphi}]+$ $+\sqrt{\left(\frac{\alpha}{2}\right)^2[Q^{-2}-2Q^{-1}E_0^{s\varphi}]-Q^{-1}E_0^{s\varphi}}$	$E_0^{s\varphi}$[b]
$Q^{-1}\delta^2 \gg 1$[a], $R \ll 1$	(6.8)	(6.2)[c]	
$Q^{-1}\delta^2 \gg 1$[a], $R \ll 1$, $\sqrt{Q}R/\alpha \gg 1$[d]	$\frac{4\sqrt{3}}{\pi^{3/2}}\sqrt{Q^{-1}}R^{7/2}$ (6.10)	$\sqrt{3Q^{-1}}R$ (6.9)	$-3R^2$ (6.5)
$Q^{-1}\delta^2 \gg 1$[a], $R \ll 1$, $\sqrt{Q}R/\alpha \ll 1$[e]	$\frac{12}{\pi^{3/2}}\left(\alpha+\alpha^{-1}\right)R^{9/2}$ (6.11)	$3\left(\alpha+\alpha^{-1}\right)R^2$ (6.9)	
(*ii*) $R \gg 1$	$\frac{4\lambda_+}{\pi^{3/2}}\tanh^{3/2}R\sinh R$ $\times[\sqrt{Q}+\sqrt{1+Q}]^2$ (6.7)	$-\frac{\alpha}{2}[Q^{-1}+E_0^{s\varphi}]+$ $+\sqrt{\left(\frac{\alpha}{2}\right)^2[Q^{-2}-2Q^{-1}E_0^{s\varphi}]-Q^{-1}E_0^{s\varphi}}$ (6.2)	$-8e^{-2R}$ (4.26)
$R \gg 1$, $\sqrt{Q}e^{-R}/\alpha \ll 1$[e]	$\frac{16}{\pi^{3/2}}(\alpha+\alpha^{-1})e^{-R}$ $\times[\sqrt{Q}+\sqrt{1+Q}]^2$ (6.7)	$8(\alpha+\alpha^{-1})e^{-2R}$ (6.2)[d]	

[a] In this limit, $\det\mathcal{H}^{mp}/\det\mathcal{H}^{sp} = 1$; cf. (4.31).
[b] Has to be evaluated numerically.
[c] Compared to (6.2), small terms of the order $\mathcal{O}((QE_0^{s\varphi})^2)$ have been dropped.
[d] Typically realized in experiments.
[e] For $\alpha \to \infty$, these results merge into (5.5), (5.3) obtained in the overdamped limit.

The transition rate from the metastable state (neglecting transitions that lead back from the metastable state over the barrier to the initial state) can then be calculated as in the Appendix with the result

$$\Gamma_{\mathrm{dSG}} = \frac{\tilde{\lambda}_+}{\sqrt{2\pi^3}} \sqrt{\mathcal{E}_s} L \sqrt{\tilde{\beta}} \sqrt{\frac{\det \mathcal{H}^{m\varphi}}{\det' |\mathcal{H}^{s\varphi}|}} e^{-\tilde{\beta}\mathcal{E}_s}, \qquad (7.4)$$

where $\mathcal{E}_s$ is given by (2.15). In (7.4) a factor of 2 has been included due to the existence of two equivalent saddle points $\pm\phi_s$, and the ratio of the determinants has been calculated in (4.55). $\tilde{\lambda}_+ > 0$ is the nucleus decay frequency which is obtained by insertion of $\varphi = e^{\tilde{\lambda}_+ t}\varphi_+$ into (7.3),

$$\tilde{\lambda}_+ = \frac{\alpha Q^{-1}}{2}[-1 + \sqrt{1 + 4Q|E_0^{s\varphi}|/\alpha^2}], \qquad (7.5)$$

with $E_0^{s\varphi}$ the (negative) ground state energy of $\mathcal{H}^{s\varphi}$. Equations (7.4), (7.5) constitute the creation rate of kink-antikink pairs in the moderately damped double sine-Gordon system.

It may now be verified that the magnetization reversal rate (3.11), (3.12) with (4.31) is equivalent to the result (7.4) in the limit $Q^{-1}\delta^2 \to \infty$, provided that the time scale in (7.1)–(7.4) is chosen as $[t] = M_0/(2\gamma K_e)$ while energies and lengths are chosen as in (2.4). Taking the limit $Q|E_0^{s\varphi}|/\alpha^2 \to 0$ in (6.2) and (7.5) we obtain $\lambda_+ = (\alpha + \alpha^{-1})|E_0^{s\varphi}|$ and $\tilde{\lambda}_+ = |E_0^{s\varphi}|/\alpha$, respectively. Reinstating units, the equivalence of Γ and Γ_{dSG} is immediately verified.

VIII. DISCUSSION

In the previous sections we have investigated the rate of magnetization reversal in an effectively 1D ferromagnet which describes magnetization configurations in an ideal elongated particle of a small constant cross section $\mathcal{A}$. The experimentally most important conclusion is the existence of a saddle point structure which is *localized* along the sample. Unlike the Néel-Brown theory[2] which leads to a barrier energy $VK_e(1-h)^2$ proportional to the particle volume V, the present theory leads to an energy barrier $\mathcal{A}\mathcal{E}_s$ that is proportional to the sample cross section and to the domain-wall energy [after reinstating the units (2.4)]. For sufficiently elongated particles the energy of the nonuniform barrier is thus always lower than that of the uniform one and thus the present theory predicts much lower coercivities than the Néel-Brown theory. To illustrate this, we consider the following typical material parameters of particles such as CrO_2: $A = 5 \times 10^{-7}$ erg/cm, $K_e = 7 \times 10^5$ erg/cm^3, $M_0 = 480$ Oe, $\gamma = 1.5 \times 10^7$ Oe^{-1} s^{-1}. For $T = 300$ K, $Q^{-1} = 0.2$, $\alpha = 0.05$, the numerically evaluated switching rate (3.11), (4.58) is shown in Fig. 6 as a function of the external field for various particle diameters but for a fixed aspect ratio of 15:1. The dotted lines represent the predictions[28] of the Néel-Brown theory, while $H_{\mathrm{ext}}M_0/(2K_e) = 1$ is the Stoner-Wohlfarth value[43] of the nucleation field. One clearly recognizes the significant coercivity reduction for particles with small diameters. Note that the switching rate at a given field predicted by the present theory exceeds that of the Néel-Brown theory by more than ten orders of magnitude. Conversely, the coercivity of a particle of diameter 100 Å exhibits a coercivity which (depending on the measurement time) is about one-third of the Stoner-Wohlfarth value. Since the barrier energy $\mathcal{A}\mathcal{E}_s$ is independent of the particle length, the present theory predicts the coercivity to become independent of the particle length for sufficiently long particles. This is in contrast to the theory of Néel and Brown which predicts a suppression of thermal effects in the particle volume.

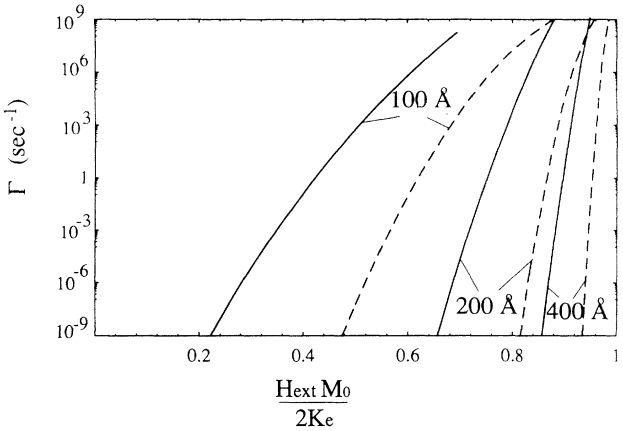

FIG. 6. The total nucleation rate Γ is shown as a function of the reduced external field for various particle diameters. The material parameters are chosen as in Sec. VIII. The dashed curves indicate the results of the Néel-Brown theory. The particle aspect ratio is assumed to be 15:1.

Experiments investigating the coercivity of a single elongated particle indeed show a significant coercivity reduction from the Stoner-Wohlfarth value for fields along the particle. These experiments have also shown an asymmetry in the angular dependence of the coercivity, the coercivity reduction being more pronounced for external fields along the particle axis than for fields directed perpendicularly to the sample. Both of these findings are in qualitative agreement[42] with the present theory. A quantitative comparison between theory and experiments is difficult for the presently available experimental data since the particles are irregularly shaped and often contain voids. Experiments on particles with a more perfect morphology such as CrO_2 or data of particles with various aspect ratios and diameters would clearly be desirable to further clarify the mechanism of thermally activated magnetization reversal.

Let us now recall the various assumptions that have been made in the present theory:

The cross sectional area has been considered constant throughout the particle. This assumption leads to a continuous degeneracy of the solution ϕ_s with respect to translations. In the case of a varying cross sectional area, the present treatment will still be approximately correct if the variations have a much shorter wavelength than

the characteristic length scale δ of the nucleus. However, if the cross sectional area varies substantially, the saddle point energy will depend on the coordinate x_0 in (2.9) and hence a whole class of energetically almost degenerate saddle points emerge. Such an extension of the present theory would predict that one single particle behaves as if there would be a distribution of saddle point energies. Experimental results[44] indeed show deviations from an Arrhenius law involving a single energy barrier. They exhibit a decay of the magnetic moment of a single particle that is proportional to $\ln t$ over several decades in t, a fact that is usually attributed to a distribution of energy barriers. Such a behavior cannot be reconciled with the simple Néel-Brown picture which predicts a unique energy barrier for a single particle.

In addition, we have focused on nucleation in the interior of the particle but we have neglected effects occurring at the particle ends. Since the nucleus ϕ_s describes a magnetization configuration merging asymptotically into the metastable state, the present nucleus may also be used to describe a situation where the magnetization is pinned at the sample ends. In order for the present theory to hold, however, the pinning energy has to be sufficiently small that it can be overcome by the two domain walls propagating from the nucleation location to the sample ends.

In the opposite case of free boundary conditions, i.e., $\mathbf{M}'(\pm L/2) = 0$, there exists also the possibility that only one domain wall is nucleated at one sample end. This case can also be related to the present theory. In the ideal situation of a sample of constant cross section and an effective easy-axis anisotropy that extends to the sample end (at least within a distance smaller than the domain-wall width), the saddle point structure ϕ_s restricted to the interval $-\infty < x < 0$ represents a domain wall which is nucleated at the sample end $x = 0$. Consequently the corresponding energy is half of the nucleus energy $\mathcal{A}\mathcal{E}_s$.

The theory as outlined in the Appendix applies to the regime of moderate to large friction. Since, however, the damping constant in magnetic systems is quite small, some estimates of the applicability range of the present theory are presented in the following.

A. Validity of the theory

The principal existence of a lower limit of the damping constant for the present theory may be seen as follows. For $\alpha = 0$, the linearized equations (3.1) do not describe the decay of the nucleus towards the stable state but rather a purely precessional motion which conserves the energy. Therefore, the corresponding decay frequency λ_+ is completely irrelevant for the nucleation rate for $\alpha \to 0$.

For very small values of the damping constant α, a completely different methodology would have to be applied, since the nucleation no longer corresponds to a diffusion in configuration space but rather in energy space. Since the time evolution of the nucleus for extremely small α is expected to exhibit a "breathing" oscillation,[45] a derivation of the corresponding Fokker-Planck equation would be an extremly difficult task. However, we shall see that the applicability range of the present theory extends to rather small values of α even for small nuclei and small cross sectional areas of the sample. Therefore we do not consider the underdamped theory any further.

A criterion for the crossover between the present theory and energy diffusion has been given by Landauer and Swanson[14] (see also Ref. 16 and Ref. 39). The moderately damped theory may be applied if the energy loss during an (approximate) period of the motion near the saddle point exceeds k_BT.

Using the equations of motion (2.2) we obtain for the energy loss rate per area

$$\frac{d\mathcal{E}}{dt} = -\alpha \int dx\, (\partial_t \mathbf{m})^2 , \tag{8.1}$$

where $\mathbf{m} \equiv \mathbf{M}/M_0$. Since (8.1) may also be expressed by spatial instead of temporal derivatives, it is clear that the energy loss will be smallest for small nuclei. In this limit we may employ the spin-wave approximation $m_y, m_z \ll 1$, $m_x = -1 + \mathcal{O}(m_x^2)$. The energy loss during one approximate period then takes the form

$$\mathcal{A}\Delta\mathcal{E} = -\alpha\mathcal{A} \int_0^{\frac{2\pi}{\omega}} dt \int dx \left\{ (\partial_t m_y)^2 + (\partial_t m_z)^2 \right\} , \tag{8.2}$$

where $\frac{2\pi}{\omega}$ is the precession period. The rhs of (8.2) is now evaluated approximately. First, we are only interested in leading order in α and thus we may use the conservative equations of motion for the evaluation of the integrand in (8.2). Second, we discard any breathing effects and neglect the exchange coupling of the magnetic moments such that the precession amplitude is given by the spatial distribution of the nucleus. Linearization of the equations of motion for $\alpha = 0$, $\partial_t \mathbf{m} = \mathbf{m} \times (\partial \mathcal{E}_0 / \partial \mathbf{m})$, with $\mathcal{E}_0$ the energy (2.1) without exchange, then leads to

$$\begin{aligned} \partial_t m_y &= (1 - h + Q^{-1}) m_z , \\ \partial_t m_z &= -(1-h) m_y . \end{aligned} \tag{8.3}$$

They describe an elliptical precession $m_z = m_z^0 \sin \omega t$, $m_y = -m_y^0 \cos \omega t$ with $m_z^0/m_y^0 = \sqrt{1-h}/\sqrt{1-h+Q^{-1}}$ and $\omega = \sqrt{(1-h)(1-h+Q^{-1})}$. Inserting this into (8.2) we obtain

$$\mathcal{A}\Delta\mathcal{E} = -\alpha\mathcal{A}\frac{2\pi}{\omega} \int dx (m_y^0)^2 (1-h) \left(1 - h + \frac{Q^{-1}}{2} \right) . \tag{8.4}$$

Now, for small nuclei, we have $h = \operatorname{sech}^2 R \simeq 1 - R^2$. The precession is assumed to cover the nucleus structure and therefore we have $m_y^0 = 2 \sinh R \cosh(x/\delta) / [\sinh^2 R + \cosh^2(x/\delta)]$. Inserting this in (8.4) and performing the integration the validity condition $\mathcal{A}\Delta\mathcal{E} > k_BT$ takes the following form in leading order R:

$$\Delta\mathcal{E} = 8\pi Q^{-1/z2} \beta \mathcal{A} \alpha R^2 > 1. \tag{8.5}$$

For typical values of the constants as given above and $Q^{-1} = 0.2$ we obtain the condition $\alpha R^2 a\ 7 \times 10^{13} > 1$ where a is the cross section area measured in cm^2. The

limit is reached for, e.g., $\alpha = 0.05$, $R = 0.4$ ($h = 0.84$) at particle diameters 70 Å. Note that due to the neglection of the breathing contribution to the energy loss this represents a lower limit for α and therefore the theory may be applied even for smaller values of α or samples smaller than indicated above.

ACKNOWLEDGMENTS

I kindly acknowledge illuminating discussions with W. Baltensperger, S. Skourtis, H. Suhl, and P. Talkner. This work was supported by the Swiss National Science Foundation and by ONR-Grant No. N00014-90-J-1202.

APPENDIX

In this appendix we present a derivation of the expression for the nucleation rate starting from the Fokker-Planck equation (3.8) near the saddle point. Since the deterministic part of the dissipative linearized equations (3.2) constitutes a non-Hermitian eigenvalue problem, there is no known set of eigenfunctions to expand in and therefore traditional formulations which are based on an expansion into mode amplitudes cannot be applied immediately. In the sequel we shall show, however, that the within a functional formulation, the derivation of the nucleation rate can be carried out in close analogy to the methods of Kramers[13] and its extension to many degrees of freedom by Langer.[7(b)] In the limit of large friction the result reduces to the theories[14] of Brinkman, Landauer-Swanson, and Langer.

The basic principles of the method go back to Kramers.[13] We calculate the stationary flux of a nonequilibrium distribution across a surface transverse to the unstable direction at the saddle point. A main difference to finite dimensional problems is the existence of the Goldstone mode with zero energy which reflects the continuous degeneracy of the nucleus ϕ_s with respect to rigid translations.

Our goal is the construction of a *stationary nonequilibrium* probability density obeying the boundary conditions $\varrho \simeq 1$ near the metastable state and $\varrho \simeq 0$ beyond the saddle point. To this end we factorize the desired probability distribution as follows:

$$\varrho = \varrho_{\rm eq} F. \tag{A1}$$

The key assumption is now to let F be a function of one coordinate u only. F is such that ϱ is a normalizable function. In the vicinity of the saddle point, the coordinate u is a linear functional in ψ,

$$u = \int dx \sum_j U_j(x)\psi_j(x), \tag{A2}$$

with $(U_1, U_2) = (U^\varphi, U^p)$. After insertion of (A1) with (A2) into (3.8) and using the stationarity of ϱ we obtain

$$\int dx \sum_{ij} M_{ij}\left[-\mathcal{H}_i\psi_i(x)U_j(x)\frac{dF}{du} + \frac{1}{\beta\mathcal{A}}U_i(x)U_j(x)\frac{d^2F}{du^2}\right] = 0. \tag{A3}$$

In order for (A3) to become a proper differential equation in u alone we must have

$$\int dx \sum_{ij} M_{ij}\mathcal{H}_i\psi_i(x)U_j(x) = \kappa u, \tag{A4}$$

$$\frac{1}{\beta\mathcal{A}}\int dx \sum_{ij} M_{ij}U_i(x)U_j(x) = \gamma\kappa, \tag{A5}$$

where γ, κ are real constants. Since from (3.5), $\sum_{ij} M_{ij}U_iU_j = \alpha\sum_i U_i^2$, the condition (A5) amounts to a normalization of the U_i, and we have $\gamma\kappa > 0$. Using (A4) and (A5), Eq. (A3) reduces to the same differential equation as in the case[13] of one degree of freedom:

$$-u\frac{dF}{du} + \gamma\frac{d^2F}{du^2} = 0, \tag{A6}$$

which is integrated with the boundary conditions $F(-\infty) = 1$, $F(\infty) = 0$; i.e., the vicinity of the metastable state ($u \to -\infty$) is characterized by thermal equilibrium while the probability distribution vanishes beyond the sadlle point ($u \to \infty$). Since ϱ has to be normalizable, we must have $\gamma < 0$ and hence $\kappa < 0$. F is then given by

$$F(u) = \frac{1}{\sqrt{2\pi|\gamma|}}\int_u^\infty du \exp\left\{-\frac{u^2}{2|\gamma|}\right\}. \tag{A7}$$

Inserting (A7) and (A5) into (3.9) we obtain for the current near the saddle point

$$J_i(x) = \frac{1}{\beta\mathcal{A}\sqrt{2\pi|\gamma|}}\exp\left\{-\frac{u^2}{2|\gamma|}\right\}\varrho_{\rm eq}\sum_j M_{ij}U_j(x). \tag{A8}$$

We now return to the evaluation of κ. Equation (A4) is fulfilled if

$$\sum_j M_{ij}\mathcal{H}_iU_j = \kappa U_i. \tag{A9}$$

Note that this implies that $U^\varphi(x)$ has no component along the zero frequency mode since $(\chi_1^{s\varphi}, U^\varphi) = \kappa^{-1}\sum M_{\varphi j}\,(\mathcal{H}^{s\varphi}\chi_1^{s\varphi}, U^\varphi) = 0$. This is physically plausible since the dynamical instability of ϕ_s is only associated with a shrinking or expansion of the nucleus but *not* with a pure translation of the nucleus as described by $\chi_1^{s\varphi}(x)$. Because $\mathcal{H}^{sp}$ is a positive operator, there is no restriction on the functions $U^p(x)$. Therefore (A9) can be inverted to give

$$\sum_j M_{ij}U_j = \kappa\mathcal{H}_i^{-1}U_i, \tag{A10}$$

where $(\mathcal{H}^{s\varphi})^{-1}$ acts only on the subspace $\{f|(f,\chi_1^{s\varphi}) = 0\}$. Equation (A10) and hence (A9) are solved by putting $U_i = \mathcal{H}_i\psi_i^+$ where $\psi^+ = (\varphi_+, p_+)$ is the dynamical unstable mode obeying (3.2). Therefore we have

$$\kappa = -\lambda_+ < 0. \tag{A11}$$

The escape rate Γ is now obtained by integrating the flux transverse to the unstable direction, e.g., over the manifold $u = 0$:

$$\Gamma = \int_{u=0} \mathcal{D}\varphi\mathcal{D}p \int dx \sum_i U_i(x)J_i(x)$$
$$= \lambda_+\sqrt{\frac{|\gamma|}{2\pi}} \int \mathcal{D}\varphi\mathcal{D}p\,\delta(u)\,\varrho_{\rm eq}, \tag{A12}$$

where we have used (A8) and λ_+ is determined by the eigenvalue equation (3.2). The constant γ will cancel in the final result as we shall see below. $\varrho_{\rm eq}$ has to be evaluated on the hyperplane $u = 0$ in the vicinity of the saddle point. According to (3.10) it is given by $\varrho_{\rm eq} = \exp\{-\beta\mathcal{A}\mathcal{E}_s^{(2)}\}/Z$ with Z determined by the normalization of $\varrho_{\rm eq}$ in the vicinity of the metastable state. Upon insertion of (3.10) and using the Fourier representation of the δ function, Eq. (A12) reads

$$\Gamma = \lambda_+\sqrt{\frac{|\gamma|}{2\pi}}\frac{e^{-\beta\mathcal{A}\mathcal{E}_s}}{Z}\int\frac{dq}{2\pi}\int\mathcal{D}\varphi\,\mathcal{D}p\,\exp\{iqu\}$$
$$\times\exp\left\{-\beta\mathcal{A}\left[\frac{1}{2}\int dx\varphi\mathcal{H}^{s\varphi}\varphi + \frac{1}{2}\int dxp\mathcal{H}^{sp}p\right]\right\}. \tag{A13}$$

For the evaluation of the functional integrals we use the self-adjointness of $\mathcal{H}^{s\varphi}$ and $\mathcal{H}^{sp}$ acting on functions with periodic boundary conditions on $[-\frac{L}{2}, \frac{L}{2}]$. Therefore they have an orthogonal and complete set of eigenfunctions $\chi_\nu^{s\varphi}, \chi_\nu^{sp}$ with $\mathcal{H}^{s\varphi}\chi_\nu^{s\varphi} = E_\nu^{s\varphi}\chi_\nu^{s\varphi}$, $\mathcal{H}^{sp}\chi_\mu^{sp} = E_\mu^{sp}\chi_\mu^{sp}$, where ν, μ denote the bound states $\nu, \mu = 0, 1, (2)$ and scattering states $\nu, \mu = k$ as well. Therefore we can expand

$$\varphi(x) = \sum_\nu \varphi_\nu\,\chi_\nu^{s\varphi}(x), \tag{A14}$$

$$p(x) = \sum_\mu p_\mu\,\chi_\mu^{sp}(x), \tag{A15}$$

where $\chi_{-k} = \chi_k^*$, and φ_ν, p_ν are complex expansion coefficients. Since φ and p are real, we have $\varphi_\nu = \varphi_{-\nu}^*$ and $p_\nu = p_{-\nu}^*$. Expanding similarly $u = \sum U_\nu^{\varphi\,*}\varphi_\nu + \sum U_\mu^{p\,*}p_\mu$ we obtain

$$\Gamma = \lambda_+\sqrt{\frac{|\gamma|}{2\pi}}\frac{e^{-\beta\mathcal{A}\mathcal{E}_s}}{Z}\int\frac{dq}{2\pi}\int\prod_\nu d\varphi_\nu\int\prod_\mu dp_\mu$$
$$\times\exp\left\{\sum_\nu{}'\left(iqU_\nu^{\varphi\,*}\varphi_\nu - \frac{\beta\mathcal{A}}{2}E_\nu^{s\varphi}\varphi_\nu^*\varphi_\nu\right)\right\}$$
$$\times\exp\left\{\sum_\mu\left(iqU_\mu^{p\,*}p_\mu - \frac{\beta\mathcal{A}}{2}E_\mu^{sp}p_\mu^*p_\mu\right)\right\}, \tag{A16}$$

where the prime on the sum indicates that the integrand is independent of φ_1, since $E_1^{s\varphi} = U_1^\varphi = 0$. To simplify notation we now choose integration measures $(d\varphi_\nu)$ and (dp_μ) in (A16) *and* in Z such that, e.g.,

$$\int_{-\infty}^{\infty}(dp_0)\exp\left\{-\frac{\beta\mathcal{A}}{2}E_0^{sp}p_0^2\right\} = \frac{1}{\sqrt{E_0^{sp}}},$$
$$\int_{-\infty}^{\infty}(dp_k^*)(dp_k)\exp\{-\beta\mathcal{A}E_k^{sp}p_k^*p_k\} = \frac{1}{E_k^{sp}}. \tag{A17}$$

But note that we have to restore $\sqrt{\beta\mathcal{A}/2\pi}$ in the integration over the zero mode which does not contain a Gaussian and note also that the integration measure in q is the usual one. We now perform the integrations in φ_ν and p_μ except for the amplitudes of the zero mode φ_1 and that of the unstable mode, φ_0, to obtain

$$\Gamma = \lambda_+\sqrt{\frac{|\gamma|}{2\pi}}\frac{e^{-\beta\mathcal{A}\mathcal{E}_s}}{Z}\frac{1}{\sqrt{\det''\mathcal{H}^{s\varphi}}}\frac{1}{\sqrt{\det\mathcal{H}^{sp}}}\int(d\varphi_1)$$
$$\times\int(d\varphi_0)\int\frac{dq}{2\pi}\exp\left\{-\frac{q^2}{2\beta\mathcal{A}}\left(\sum_\nu{}''\frac{|U_\nu^\varphi|^2}{E_\nu^{s\varphi}}\right.\right.$$
$$\left.\left.+\sum_\mu\frac{|U_\mu^p|^2}{E_\mu^{sp}}\right)\right\}$$
$$\times\exp\left\{iqU_0^\varphi\varphi_0 + \frac{\beta\mathcal{A}}{2}|E_0^{s\varphi}|\varphi_0^2\right\}. \tag{A18}$$

The expression $\det\mathcal{H}$ stands for the product of all eigenvalues of $\mathcal{H}$. The double prime on the determinant and the summation indicates that the terms $\nu = 0, 1$ corresponding to the unstable mode and the zero mode, are omitted.

We now turn to the evaluation of the zero mode. To this end we remember that a pure translation of the nucleus can be described by $\phi_s(x + dx) - \phi_s(x) = \phi_s'(x)dx$ or since $\chi_1^{s\varphi} \propto d\phi_s/dx$ we can equally well write $\phi_s(x+dx)-\phi_s(x) = \chi_1^{s\varphi}(x)\,d\varphi_1$. This allows us to replace the integration over the zero mode by an integration over x. Since $\chi_1^{s\varphi}$ is normalized to unity and reinstating the integration measure (A17) of $(d\varphi_1)$ we have

$$\int(d\varphi_1) = \sqrt{\frac{\beta\mathcal{A}}{2\pi}}\int_{-L/2}^{L/2}dx\sqrt{\int dx'\left[\frac{d\phi_s}{dx'}\right]^2} = \sqrt{\frac{\beta\mathcal{A}}{2\pi}}\mathcal{L}, \tag{A19}$$

where

$$\mathcal{L} \equiv \sqrt{\mathcal{E}_s}L. \tag{A20}$$

Here we have made use of (2.15). After performing the q integration (A18) we have to convince ourselves that the remaining integral converges. This is ensured by the following relation, which follows from (A5) and (A10):

$$\sum_i\int dxU_i(x)\mathcal{H}_i^{-1}U_i(x) = -|\gamma|\beta\mathcal{A} < 0. \tag{A21}$$

Using the expansions of U_i in terms of the $\chi_\nu^{s\varphi,p}$ and recalling that $U_1^\varphi \equiv 0$ we see that the exponent is in fact negative. We are now left with the evaluation of Z.

Since $\varrho_{\rm eq}$ is strongly peaked at the metastable state we can perform a Gaussian approximation

$$Z = \int \mathcal{D}\varphi\, \mathcal{D}p \exp\left\{-\beta\mathcal{A}\left[\frac{1}{2}\int dx\, \varphi\, \mathcal{H}^{m\varphi}\, \varphi + \frac{1}{2}\int dx\, p\, \mathcal{H}^{mp}\, p\right]\right\}, \tag{A22}$$

where in contrast to the above φ and p now describe fluctuations out of the *metastable* state. They are defined by $\phi = \pi + \varphi$ and $\theta = \pi/2 - p$, where $|\varphi|, |p| \ll 1$. This integral is performed analogously to the previous one: φ and p may be expanded into the (plane wave) eigenstates of $\mathcal{H}^{m\varphi}, \mathcal{H}^{mp}$. The integrations then are all Gaussian and using the measure (A17) for the integrations, we finally obtain

$$Z = \frac{1}{\sqrt{\det \mathcal{H}^{m\varphi}}}\frac{1}{\sqrt{\det \mathcal{H}^{mp}}}. \tag{A23}$$

After having performed the q integration we can now carry out the final Gaussian integration over the unstable mode φ_0. Using (A5), (A18) leads to the final result

$$\Gamma = \frac{\lambda_+}{2\pi}\mathcal{L}\sqrt{\frac{\beta\mathcal{A}}{2\pi}}\sqrt{\frac{\det \mathcal{H}^{m\varphi}}{\det' |\mathcal{H}^{s\varphi}|}}\sqrt{\frac{\det \mathcal{H}^{mp}}{\det \mathcal{H}^{sp}}}e^{-\beta\mathcal{A}\mathcal{E}_s}, \tag{A24}$$

where $\det' |\mathcal{H}^{s\varphi}|$ denotes the product of the modulus of the eigenvalues with omission of the zero mode. Apart from the dynamical prefactor the result *looks as if* we had evaluated in Gaussian approximation the ratio Z_m/Z_s of the partition functions at the metastable state and the saddle point, respectively, with the unstable rendered into a stable one. Or loosely speaking, the nucleation rate is proportional to the imaginary part of the ratio Z_m/Z_s. For later reference, we express the result (A24) in terms of the eigenvalues $E_\nu^{s\varphi}, E_\mu^{sp}$:

$$\Gamma = \frac{\lambda_+}{2\pi}\mathcal{L}\sqrt{\frac{\beta\mathcal{A}}{2\pi}}\frac{1}{\sqrt{|E_0^{s\varphi}|E_2^{s\varphi}E_0^{sp}E_1^{sp}}} \times\sqrt{\frac{\Pi k_1 E_{k1}^{m\varphi}}{\Pi k_1' E k_1'^{\,s\varphi}}}\sqrt{\frac{\Pi k_2 E_{k2}^{mp}}{\Pi k_2' E k_2^{sp}}}e^{-\beta\mathcal{A}\mathcal{E}_f}, \tag{A25}$$

where according to (A20) $\mathcal{L} = L\sqrt{\mathcal{E}_s}$ [$\mathcal{E}_s$ is given by (2.15)] and λ_+ is determined by (3.2). Note that in our case of two equivalent saddle points $\phi^\pm$ we have to multiply this final result by a factor of 2.

* Present address: electronic address: hbraun@sfu.ca

[1] See, e.g., J.F. Dillon, in *Magnetism*, edited by G.R. Rado and H. Suhl (Academic, New York, 1963), Vol. III, and references therein.
[2] L. Néel, Ann. Geophys. **5**, 99 (1949).
[3] W.F. Brown, Phys. Rev. **130**, 1677 (1963); IEEE Trans. Magn. **MAG-15**, 1196 (1979).
[4] H.B. Braun, Phys. Rev. Lett. **71**, 3557 (1993).
[5] J.S. Broz, H.B. Braun, O. Brodbeck, W. Baltensperger, and J.S. Helman, Phys. Rev. Lett. **65**, 787 (1990).
[6] H.B. Braun, preceding paper, Phys. Rev. B **50**, 16 485 (1994).
[7] (a) J.S. Langer, Ann. Phys. (N.Y.) **41**, 108 (1967); (b) **54**, 258 (1969).
[8] D.E. McCumber and B.I. Halperin, Phys. Rev. B **1**, 1054 (1970).
[9] B.V. Petukhov and V.L. Pokrovskii, Sov. Phys. JETP **36**, 336 (1973).
[10] M. Büttiker and R. Landauer, Phys. Rev. A **23**, 1397 (1980).
[11] G. Barton, J. Phys. A **18**, 479 (1985).
[12] R.G. Newton, J. Math. Phys. **24**, 2152 (1983).
[13] H.A. Kramers, Physica **7**, 284 (1940).
[14] H.C. Brinkman, Physica **22**, 149 (1956); R. Landauer and J.A. Swanson, Phys. Rev. **121** (1961); J.S. Langer, Phys. Rev. Lett. **21**, 973 (1968).
[15] S. Coleman, Phys. Rev. D **15**, 2929 (1977); C.G. Callan and S. Coleman, *ibid.* D **16**, 1762 (1977).
[16] P. Hänggi, P. Talkner, and M. Borkovec, Rev. Mod. Phys. **62**, 251 (1990).
[17] A. Aharoni, Phys. Rev. **135**, A447 (1964).
[18] I. Eisenstein and A. Aharoni, Phys. Rev. B **14**, 2078 (1976).
[19] M. Enz and R. Schilling, J. Phys. C **19**, 1765 (1986).
[20] J.L. van Hemmen and S. Sütö, Europhys. Lett. **1**, 481 (1986); Physica **141B**, 37 (1986).
[21] E.M. Chudnovsky and L. Gunther, Phys. Rev. B **37**, 9455 (1988).
[22] A. Garg and G.-H. Kim, Phys. Rev. Lett. **63**, 2512 (1989).
[23] D.D. Awschalom, J.F. Smyth, G. Grinstein, D.P. DiVincenzo, and D. Loss, Phys. Rev. Lett. **68**, 3092 (1992).
[24] D. Loss, D.P. DiVincenzo, and G. Grinstein, Phys. Rev. Lett. **69**, 3232 (1992).
[25] E.M. Chudnovsky and L. Gunther, Phys. Rev. Lett. **60**, 661 (1988).
[26] A.O. Caldeira and K. Furuya, J. Phys. C **21**, 1227 (1988).
[27] P.C.E. Stamp, E.M. Chudnovsky, and B. Barbara, Int. J. Mod. Phys. B **6**, 1355 (1992).
[28] I. Klik and L. Gunther, J. Stat. Phys. **60**, 473 (1990).
[29] Note, however, that the existence of a saddle point of curling symmetry does not ensure the possibility of magnetization reversal within a continuum model. For topological reasons due to the "backbone" at the cylinder axis, the magnetization along an infinite cylinder cannot be reversed via configurations that are always tangential to the sample surface. While this argument prohibits the existence of "curling" nuclei for small particles with diameter of less than a domain-wall width, the discreteness of the lattice reduces the above topological barrier for large sample diameters such that saddle points of "curling symmetry," which are localized along the particle, are indeed expected to be the relevant energy barriers.
[30] J.S. Broz, Ph.D. thesis, ETH Zürich, 1990; J.S. Broz and W. Baltensperger, Phys. Rev. B **45**, 7307 (1992).
[31] A. Aharoni and W. Baltensperger, Phys. Rev. B **45**, 9842 (1992).
[32] An estimate for this crossover to a one-dimensional behavior may also be obtained by comparing energies of the "curling" (vortex) configuration $\mathbf{M}/M_0 = (\sin\phi, \cos\phi, 0)$

and the uniform distribution $\mathbf{M} = M_0\mathbf{e}_x$ in an infinite cylinder of radius R and lattice constant a. For vanishing hard-axis anisotropy ($K_h = 0$), the former configuration has exchange energy $2\pi A \ln(R/a)$ but the corresponding demagnetizing field [cf. (2.3) of paper I] is zero due to the absence of magnetic poles. On the other hand, the uniform configuration has vanishing exchange energy but demagnetizing energy $\pi^2 R^2 M_0$ due to surface poles. The uniform configuration is therefore energetically favorable for sufficiently small radii such that $R^{-2}\ln(R/a) > \pi M_0^2/(2A)$.

[33] F.H. Leeuw, R. van den Doel, and U. Enz, Rep. Prog. Phys. **43**, 690 (1980).

[34] J. Zinn-Justin, *Quantum Field Theory and Critical Phenomena* (Clarendon, Oxford, 1993), Chap. 4.2.

[35] R. Rajaraman, *Solitons and Instantons* (North-Holland, Amsterdam, 1982).

[36] L.S. Schulman, *Techniques and Applications of Path Integration* (Wiley, New York, 1981).

[37] Note that Ref. 11 deals with zero boundary conditions, i.e., $\chi(-L/2) = \chi(L/2) = 0$, which leads to a shift of the spectrum of even eigenfunctions by $\Delta k = \pi/L$ compared to periodic boundary conditions as considered here. The spectrum of odd-parity eigenfunctions is identical for periodic and zero boundary conditions.

[38] A zero energy resonance occurs if the Jost function for even or odd parity is zero for $k = 0$.

[39] The functions χ_1^{sp}, ξ_1^{sp} should be replaced by χ_0^{sp}, ξ_0^{sp} respectively. However, χ_0^{sp} given by (4.41) is now a symmetric function while ξ_0^{sp} an antisymmetric function.

[40] This statement is true in the moderate to strong damping regime which is considered in the present paper. We do not consider here the underdamped regime which would require a completely different approach by constructing a Fokker-Planck equation in the energy variable. For a criterion separating these two regimes see also Sec. VIII.

[41] H.B. Braun and O. Brodbeck, Phys. Rev. Lett. **70**, 3335 (1993).

[42] E.C. Stoner and E.P. Wohlfarth, Philos. Trans. R. Soc. London A **240**, 599 (1948).

[43] H.B. Braun and H.N. Bertram, J. Appl. Phys. **75**, 4609 (1994).

[44] M. Lederman, D. R. Fredkin, R. O'Barr, S. Schultz, and M. Ozaki, J. Appl. Phys. **75**, 6217 (1994).

[45] P. Talkner and H.B. Braun, J. Chem. Phys. **88**, 7537 (1988).